ANL/CP--72421

DE91 011168

IMPLEMENTATION OF THE FLOW-MODULATED SKEW-UPWIND DIFFERENCE SCHEME IN THE COMMIX-1C CODE – A FIRST ASSESSMENT

by

M. Bottoni, T. H. Chien, H. M. Domanus, W. T. Sha, and Y. Shen
Materials and Components Technology Division
Argonne National Laboratory
9700 South Cass Avenue
Argonne, Illinois 60439

and

R. Laster
Department of Mechanical Engineering
Texas A&M University
College Station, Texas 77843

To be presented at the XIV Meeting of the Liquid Metal Boiling Working Group (LMBWG), ENEA Brasimone, April 16–18, 1991

Work sponsored by the Office of Analysis and Evaluation of Operational Data, U.S. Nuclear Regulatory Commission, Washington D. C. 20555

Contents

Figures

Table

Nomenclature

A	Area (m^2)
a_l	Coefficients in discretized momentum equation (kg/s)
$CX1_\ell$,$CX2_\ell$	Coefficients for determining face velocities in x-directions
$CY3_\ell$,$CY4_\ell$	Coefficients for determining face velocities in y-directions
$CZ5_\ell$,$CZ6_\ell$	Coefficients for determining face velocities in z-directions
D	Diffusion strength (kg/s)
f_ℓ	Weighting factor for cell ℓ
Fx	Mass flux in x-direction (kg/s)
Fy	Mass flux in y-direction (kg/s)
Fz	Mass flux in z-direction (kg/s)
g	Gravity acceleration (m/s^2)
H	Heaviside's function
p	Pressure (N/m^2)
$\vec{R}$	Drag force, resistance (kg/m^2s^2)
S	Source term (kg/m^2s^2)
T	Stress tensor (kg/ms^2)
t	Time (s)
u	x-component of velocity (m/s)
v	y-component of velocity (m/s)
$\vec{V}_\ell$	Fluid volume around node ℓ (m^3)
$\vec{V}$	Velocity vector (m/s)
w	z-component of velocity (m/s)
x,y,z	Coordinate direction (m)

Greek

δ	Difference increment of variables
Δ	Finite-difference increment of variables
μ	Dynamic viscosity (kg/m s)
ν	Kinematic viscosity (m^2/s)
ρ	Density (kg/m^3)
θ	Angle measure in radiants

Subscripts

i	Used to index cells in x-coordinate direction
j	Used to index cells in y-coordinate direction
k	Used to index cells in z-coordinate direction
o	Used to index centered cells
SUD	Skew-upwind difference formulation

Superscripts

*	Volume-averaged
r	Time-discretization index
(I)	First form
(II)	Second form

Introduction

Using the concept of feedback sensitivity in the analysis of stability behavior of discretized partial differential equations, B. P. Leonard[1] proved that central differences applied to even-order derivatives yield stable algorithms, while applied to odd-order derivatives they yield algorithms without inherent stability.

In a low-convection, diffusion-dominated flow, in which both convective and diffusive terms are discretized with central differences, the stabilizing effect of the diffusion term is sufficient to grant stability; in a flow dominated by convection, the stabilizing effect of the diffusion term becomes weaker and cannot prevent wiggles that finally lead to instability. The threshold between stable and unstable conditions is generally expressed in terms of the grid Peclet number, $Pe = u\Delta x/v$, and lays by $Pe = 2$.

For these reasons, in convective-dominated flows the upwind discretization scheme is generally used. The feedback sensitivity analysis proves its unconditional stability properties. The drawback of upwind differences is in the introduction into the numerical scheme of a false diffusion coefficient arising from the truncation error of a Taylor series expansion of the dependent variables around a given point in the space-time domain. A Fourier transform, with respect to the spatial coordinate, of the set of values representing the numerical solution at the grid points, for a given time level, yields further insight into the nature of numerical diffusion, which in fact consists of amplitude, phase, and Gibbs errors. The amplitude errors are typical of short-wavelength harmonics that are either enhanced or damped with time. Numerical results in the first case, display oscillations leading to instabilities, in the second smoothed gradients. Phase errors are typical of long-wavelength harmonics that do not travel with constant speed, but either retard or accelerate, causing a dispersion of the spectral image of the numerical solution. Gibbs errors consist of unphysical oscillations of the numerical solution between the nodes. Their ultimate cause is in the discretization process itself, which leaves the dependent variables undetermined between the nodes.

The problem of numerical diffusion was experienced first by von Neumann and Richtmyer in the numerical simulation of hydrodynamical shocks.[2] Their numerical results displayed both an oscillatory behavior and a smearing of the shock front. The numerical problem was tackled by introducing both in the energy and momentum equations describing the shock wave as a pseudo- (or artificial-) viscosity, which in the three-dimensional case has tensor character.

The advantage of the artificial viscosity method of reducing numerical diffusion is its simplicity, because the pseudotensor can be treated formally like the shear stress tensor. Its disadvantage is the requirement of very fine meshes in the transition region. Because the shock wave travels, fine meshes are required in the full computational domain, unless adaptive meshes, which travel with the shock wavem are used. Although adaptive meshes have been used in one-dimensional simulations, in the general case of three-dimensional problems they are impractical.

In case of a two-dimensional flow, it has been proved that numerical diffusion depends on the skewness of the flow with respect to the grids. It can therefore be reduced by

considering, in the differencing algorithm, upstream values of the dependent-transported variables, taken following the stream lines. Thus, not only upstream cells but also their neighboring cells are used in the differencing process. The original work in this field, pioneered by Raithby,[3] has been further refined in the work of Refs. 4 and 5.

Variants of the Skew-Upwind Difference (SUD) Scheme have been obtained by taking into account either mass flows or cell surface areas or cell volumes to weight properly the contributions of the cells involved in the discretization process. The mass-flow-weighted SUD scheme has been developed in the three-dimensional case and implemented into the energy equation of the COMMIX-1A code.[6] The volume-weighted SUD scheme was likewise implemented in the three-dimensional energy equation of the variant COMMIX-1B.[7]

Problems in the application of the SUD scheme arise when the flow is so skewed that the contributions of upwind cells become much smaller than the contributions of neighboring cells, which then must be truncated to some upper limit. This cut-off may jeopardize the convergence behavior of the scheme and lead to numerical instabilities. The problem has been tackled with the development of a new algorithm, the Flow-Modulated Skew-Upwind Difference (FMSUD) scheme, documented in Ref. 8.

An alternative strategy for reducing numerical diffusion in convection-dominated flows consists of computing the convective mass flows at the cell interfaces with both central and upwind differences and then summing them upon multiplication with suitable weights. This process is commonly referred to as linear hybridization. The convective fluxes computed with central differences are not affected by numerical diffusion, but introduce wiggles; the fluxes computed with upwind differences smooth the wiggles, but introduce numerical diffusion. Suitably weighted fluxes prevent wiggles and avoid large diffusion. The problem, however, is in finding suitable weights for all flow conditions. In the one-dimensional case, it is possible to determine weights satisfying the condition of preventing local extremes in the profile of the dependent variables. In three-dimensional cases, however, it is very arduous to satisfy this monotonicity condition for all flow situations. A tentative generalization of this approach has been made with the Filtering Remedy and Methodology (FRAM) method,[9] which is currently often associated with higher-order methods and to which reference is also made in the following.

Other approaches are the analytically laborious method of Truncation Error Cancellation (TEC),[10] in which artificial diffusion coefficients are calculated to counteract the effect of the truncation error, and in the widely used Flux Corrected Transport (FCT) method.[11] The latter consists of a predictor step, in which a first-order method is used, and of a corrector step in which a higher order scheme counteracts the effect of false diffusion by introducing antidiffusive fluxes.

Because of the difficulties inherent in the cutoff problem of SUD schemes and in the determination of corrective fluxes in methods of the FCT class, to-date numerical applications seem to favor higher-order schemes, even in three-dimensional complex computer codes. These are characterized by a quadratic, cubic, or exponential approximation of the dependent variables.

Earlier applications of higher-order approximations were reported in Refs. 12 and 13, where the Cubic Interpolated Pseudo-particle (CIP) method was applied. Although the method has been extended analytically to the three-dimensional case, so far only two-dimensional applications have been reported.

A wider range of applications has found the QUICK (Quadratic Upstream Interpolation for Convective Kinematics) method proposed by B. P. Leonard[1,14] and since documented in several publications. Although a definite assessment of the performances of the QUICK scheme (in comparison with the methods discussed earlier) is not possible at this time, it is plain that it offers the advantage of relatively simplicity because it implies the use of numerical coefficients that depend only on the geometry of the definition domain. Thus, problems related to cutoff of coefficients or to the optimization of antidiffusive fluxes, typical of methods discussed above, are overcome.

This paper explains in detail the implementation of the above-mentioned Flow-Modulated Skew-Upwind Difference (FMSUD) scheme in the momentum equation of the COMMIX-1C computer program, where the scheme has been used so far only in the energy equation. Because the three scalar components of the momentum equation are solved in different meshes, staggered with respect to the mesh used for the energy equation and displaced in the respective coordinate direction, implementation of the FMSUD scheme in the momentum equations is by far more demanding than the implementation of a single scalar equation in centered cells.

For this reason, a new approach has been devised to treat the problem, from the mathematical viewpoint, in the maximum generality and for all flow conditions, taking into account automatically the direction of the velocity vector and thus choosing automatically the weighting factors to be associated to different cells in the skew-upwind discretization. The new mathematical approach is straightforward for the treatment of inner cells of the fluid- dynamic definition domain, but particular care must be paid to its implementation for boundary cells where the appropriate boundary conditions must be applied.

The paper explains the test cases in which the implementation of the FMSUD method has been applied and discusses the quality of the numerical results against the correct solution, when the latter is known.

The paper is divided thematically in two parts. The first explains in detail the implementation of the newly devised Flow-Modulated Skew-Upwind Difference (FMSUD) scheme into the momentum equation of the COMMIX-1C computer program. This development follows the implementation of the method in the energy equation, done earlier and documented in Ref. 8. The second part describes a few test cases used to check the implementation of the FMSUD method in the code and its performances against the standard option of upwind differencing. The experience gained with the computations, though very limited in number, suggests that further work is necessary to refine the method, and, possibly, to make it a viable alternative to more widespread higher order methods.

1 Implementation of the FMSUD Scheme in the Momentum Equation of the COMMIX–1C Computer Program

1.1 Integral Form of the Momentum Equation

The momentum equation used in the COMMIX–1C program is, in tensor notation:

$$\frac{\partial}{\partial t}(\rho\vec{v}) + \nabla \cdot \rho\vec{v}\vec{v} = \nabla \cdot \underline{T} + \rho\vec{g} - \vec{R}\,, \tag{1}$$

where ρ is the density of the fluid, $\vec{v}$ is the velocity vector, $\underline{T}$ represents the stress tensor, $\rho\vec{g}$ is the body force term, and $\vec{R}$ includes all other forces acting on the fluid.

Assuming the fluid is Newtonian, we can also write Eq. 1 as

$$\frac{\partial}{\partial t}(\rho u_j) + \frac{\partial}{\partial x_\ell}(\rho u_j u_\ell) = \frac{\partial}{\partial x_\ell}\left(\mu\frac{\partial u_j}{\partial x_\ell}\right) + \rho g_j - R_j - \frac{\partial p}{\partial x_j}\,, \tag{2}$$

with x_ℓ (ℓ = 1, 2, 3) being the coordinates in three dimensions and u_j (j = 1, 2, 3) the three components of velocity vector $\vec{v}$; p is the pressure. The z-component of the momentum equation in Cartesian coordinates (x, y, z) can be written by setting $u_j = w$, and Eq. 2 gives

$$\frac{\partial}{\partial t}(\rho w) + \frac{\partial}{\partial x}(\rho uw) + \frac{\partial}{\partial y}(\rho vw) + \frac{\partial}{\partial t}(\rho ww) =$$

$$\frac{\partial}{\partial x}\left(\mu\frac{\partial w}{\partial x}\right) + \frac{\partial}{\partial y}\left(\mu\frac{\partial w}{\partial y}\right) + \frac{\partial}{\partial z}\left(\mu\frac{\partial w}{\partial x}\right) + \rho g - R_z - \frac{\partial p}{\partial z}. \tag{3}$$

The gravitation term ρg and term R_z are considered as a source term in Eq. 3 and denoted S_w; u and v are the velocities in x and y directions, respectively.

The finite-difference scheme used in COMMIX starts by dividing the flow domain into control volumes. Centered control volumes are used for scalar quantities. Staggered control volumes are constructed for velocities and mass flows. The scalar components of the momentum equation are integrated over corresponding control volumes. Integration of Eq. 3 over a w-control volume at $x = x_i$, $y = y_j$, $z = z_{K+1/2}$ yields, by means of the Gauss theorem

$$\int_{V_{f_0}} \frac{\partial}{\partial t}(\rho w)dV_f + \int_{A_{f_{i+1/2,j,k+1/2}}} (\rho uw)dA - \int_{A_{f_{i-1/2,j,k+1/2}}} (\rho uw)dA + \int_{A_{f_{i,j+1/2,k+1/2}}} (\rho vw)dA -$$

$$- \int_{A_{f_{i,j-1/2,k+1/2}}} (\rho vw) dA + \int_{A_{f_{i,j,k+1}}} (\rho ww) dA - \int_{A_{f_{i,j,k}}} (\rho ww) dA =$$

$$= \int_{A_{f_{i+1/2,j,k+1/2}}} \mu \frac{\partial w}{\partial x} dA - \int_{A_{f_{i-1/2,j,k+1/2}}} \mu \frac{\partial w}{\partial x} dA + \int_{A_{f_{i,j+1/2,k+1/2}}} \mu \frac{\partial w}{\partial y} dA -$$

$$- \int_{A_{f_{i,j-1/2,k+1/2}}} \mu \frac{\partial w}{\partial y} dA + \int_{A_{f_{i,j,k+1}}} \mu \frac{\partial w}{\partial z} dA - \int_{A_{f_{i,j,k}}} \mu \frac{\partial w}{\partial z} dA + \int_{V_{f_0}} S_w dV, \qquad (4)$$

where V_{f0} is the volume of the control cell for the z-component of the momentum equation and $A_{f_{i+1/2,j,k+1/2}}$, $A_{f_{i-1/2,j,k+1/2}}$, $A_{f_{i,j+1/2,k+1/2}}$, $A_{f_{i,j-1/2,k+1/2}}$, $A_{f_{i,j,k+1}}$, and $A_{f_{i,j,k}}$, are the faces of the control volume in x, y, and z directions, respectively.

1.2 Finite-Difference Form of the Flow-Modulated Skew-Upwinded z-Component of the Momentum Equation

The variable values at the faces of a control volume are influenced by the neighboring velocities, namely the velocities in the 26 cells surrounding the control volume.

To determine the face values, let us introduce the definition of Heaviside's function as

$$H(a) = \begin{cases} 1 & \text{if } a > 0 \\ 0 & \text{if } a \le 0 \end{cases} \qquad (5)$$

for every real number a. Hence,

$$H(-a) = 1 - H(a). \qquad (6)$$

Furthermore, the symbol [a, b] is used to define the maximum of the two real numbers a and b.

Considering the w velocity $\langle w \rangle_1 = w_{i-1/2,j,k+1/2}$ at the boundary surface between cell 0 around node (i, j, k+1/2) and cell 1, around node (i-1, j, k+1/2) (see Fig. 1), we see that if the velocity $u_{i-1/2,j,k+1/2} > 0$, the velocity $\langle w \rangle_1$ depends on w values at the left cells; if $u_{i-1/2,j,k+1/2} < 0$, $\langle w \rangle_1$ depends on w values at the right cells. Let us refer to the case of $\langle u \rangle_1 = u_{i-1/2,j,k+1/2} > 0$. Of the nine cells of the left block, only a maximum of four actually affect $\langle w \rangle_1$, depending on the sign of the velocity component $\langle w \rangle_1 = w_{i-1/2,j,k+1/2}$ and $\langle v \rangle_1 = v_{i-1/2,j,k+1/2}$ according to the following rules

If $\langle v \rangle_1 > 0$, $\langle w \rangle_1 > 0$ (cells 13, 1, 135, 15).

If $\langle v \rangle_1 < 0$, $\langle w \rangle_1 > 0$ (cells 14, 1, 145, 15).

If $\langle v \rangle_1 > 0$, $\langle w \rangle_1 < 0$ (cells 136, 1, 13, 16).

$u_1 > 0$

$CX1_1$ 136 •	$CX1_2$ • 16	$CX1_3$ • 146
$CX1_4$ 13 •	$CX1_5$ • 1	$CX1_6$ • 14
$CX1_7$ 135•	$CX1_8$ • 15	$CX1_9$ • 145

$u_1 < 0$

$CX1_1$ 36 •	$CX1_2$ • 6	$CX1_3$ • 46
$CX1_4$ 3 •	$CX1_5$ • 0	$CX1_6$ • 4
$CX1_7$ • 35	$CX1_8$ • 5	$CX1_9$ • 45

Fig. 1. Cells influencing $\langle w \rangle_1$ if $u_{1-1/2,j,k+1/2} > 0$ (left) and if $u_{1-1/2,j,k+1/2} < 0$ (right); $CX1_\ell$ (ℓ = 1, ... 9) are coefficients that take into account both weights and flow direction

If $\langle v \rangle_1 < 0$, $\langle w \rangle_1 < 0$ (cells 16, 146, 14, 1).

For all cases corresponding to $u_1 > 0$, we have

$$\begin{aligned} \langle w \rangle_1 = w_{i-1/2,j,k+1/2} = {} & CX1_1\, w_{136} + CX1_2\, w_{16} + CX1_3\, w_{146} + \\ & + CX1_4\, w_{13} + CX1_5\, w_1 + CX1_6\, w_{14} + \\ & + CX1_7\, w_{135} + CX1_8\, w_{15} + CX1_9\, w_{145}. \end{aligned} \tag{7}$$

The coefficients $CX1_\ell$ (ℓ = 1, ... 9) are defined by the following products of weighting factors and H-functions:

	$v_1, w_1 > 0$	$v_1 > 0, w_1 < 0$	$v_1 < 0, w_1 > 0$	$v_1 < 0, w_1 < 0$
$CX1_1 = f_1\, H(-w)\, H(v)$	0	f_1	0	0
$CX1_2 = f_2\, H(-w)$	0	f_2	0	f_2
$CX1_3 = f_3\, H(-w)\, H(v)$	0	0	0	f_3
$CX1_4 = f_4\, H(v)$	f_4	f_4	0	0
$CX1_5 = f_5$	f_5	f_5	f_5	f_5
$CX1_6 = f_6\, H(-v)$	0	0	f_6	f_6
$CX1_7 = f_7\, H(w)\, H(v)$	f_7	0	0	0
$CX1_8 = f_8\, H(w)$	f_8	0	f_8	0
$CX1_9 = f_9\, H(w)\, H(-v)$	0	0	f_9	0

(8)

where both velocities w and v are calculated at (i-1/2,j,k+1/2). The weighting factor f_ℓ (ℓ = 1, ... 9) satisfies the condition

$$\sum_{\ell=1}^{9} f_\ell = 1. \tag{9}$$

The values of the weighting factors f are calculated in the same way as those used in the energy equation (Ref. 8). Details of the Flow Modulated (FM) approach and of an alternative approach are given in Sec. 1.3. Similarly, for $\langle u_1 \rangle < 0$, one has

$$\begin{aligned} \langle w \rangle_1 = w_{i-1/2,j,k+1/2} = {} & CX1_1\, w_{36} + CX1_2\, w_6 + CX1_3\, w_{46} + \\ & + CX1_4\, w_3 + CX1_5\, w_0 + CX1_6\, w_4 + \\ & + CX1_7\, w_{35} + CX1_8\, w_5 + CX1_9\, w_{45}\,. \end{aligned} \tag{10}$$

Equations 7 and 10 can be combined in a single equation that holds both for $\langle u_1 \rangle > 0$ and $\langle u_1 \rangle < 0$:

$$\begin{aligned} \langle w \rangle_1 = {} & [0, \langle u \rangle_1]\, (CX1_1\, w_{136} + CX1_2\, w_{16} + CX1_3\, w_{146} + CX1_4\, w_{13} + \\ & + CX1_5\, w_1 + CX1_6\, w_{14} + CX1_7\, w_{135} + CX1_8\, w_{15} + CX1_9\, w_{145}) - \\ & - [0, -\langle u \rangle_1]\, (CX1_1\, w_{36} + CX1_2\, w_6 + CX1_3\, w_{46} + CX1_4\, w_3 + \\ & + CX1_5\, w_0 + CX1_6\, w_4 + CX1_7\, w_{35} + CX1_8\, w_5 + CX1_9\, w_{45}\,. \end{aligned} \tag{11}$$

Similarly, for the velocity component w, defined at the +x-face of the control volume, one has

$$\begin{aligned} \langle w \rangle_2 = w_{i+1/2,j,k+1/2} = {} & [0, \langle u \rangle_2]\, (CX2_1\, w_{36} + CX2_2\, w_6 + CX2_3\, w_{46} + \\ & + CX2_4\, w_3 + CX2_5\, w_0 + CX2_6\, w_4 + \\ & + CX2_7\, w_{35} + CX2_8\, w_5 + CX2_9\, w_{45}) - \\ & - [0, -\langle u \rangle_2]\, (CX2_1\, w_{236} + CX2_2\, w_{26} + CX2_3\, w_{246} + \\ & + CX2_4\, w_{23} + CX2_5\, w_2 + CX2_6\, w_{24} + \\ & + CX2_7\, w_{235} + CX2_8\, w_{25} + CX2_9\, w_{245}). \end{aligned} \tag{12}$$

The coefficients $CX2_\ell$ (ℓ = 1, ... 9) are given by the same equations (Eqs. 8), where the velocities v and w are now computed at the location i+1/2,j,k+1/2. The weights f_ℓ will also be computed according to the flow situation of the +x-face of the control volume. The above expressions can be extended to the y-direction in a similar way:

$$\begin{aligned} \langle w \rangle_3 = w_{i,j-1/2,k+1/2} = {} & [0, \langle v \rangle_3]\, (CY3_1\, w_{136} + CY3_2\, w_{36} + CY3_3\, w_{236} + \\ & + CY3_4\, w_{13} + CY3_5\, w_3 + CY3_6\, w_{23} + \\ & + CY3_7\, w_{135} + CY3_8\, w_{35} + CY3_9\, w_{235}) - \end{aligned}$$

$$- [0, -\langle v\rangle_3]\ (CY3_1\ w_{16} + CY3_2\ w_6 + CY3_3\ w_{26} +$$

$$+ CY3_4\ w_1 + CY3_5\ w_0 + CY3_6\ w_2 +$$

$$+ CY3_7\ w_{15} + CY3_8\ w_5 + CY3_9\ w_{25}) . \qquad (13)$$

$$\langle w\rangle_4 = w_{i,j+1/2,k+1/2} = [0, \langle v\rangle_4]\ (CY4_1\ w_{16} + CY4_2\ w_6 + CY4_3\ w_{26} +$$

$$+ CY4_4\ w_1 + CY4_5\ w_0 + CY4_6\ w_2 +$$

$$+ CY4_7\ w_{15} + CY4_8\ w_5 + CY4_9\ w_{25}) -$$

$$- [0, -\langle v\rangle_4]\ (CY4_1\ w_{146} + CY4_2\ w_{46} + CY4_3\ w_{246} +$$

$$+ CY4_4\ w_{14} + CY4_5\ w_4 + CY4_6\ w_{24} +$$

$$+ CY4_7\ w_{145} + CY4_8\ w_{45} + CY4_9\ w_{245}) . \qquad (14)$$

The coefficients $CY3_\ell$ are given by

	$w_3 > 0,\ u_3 > 0$	$w_3 > 0,\ u_3 < 0$	$w_3 < 0,\ u_3 > 0$	$w_3 > 0,\ u_3 < 0$	
$CY3_1 = f_1\ H(-w)\ H(u)$	0	0	f_1	0	
$CY3_2 = f_2\ H(-w)$	0	0	f_2	f_2	
$CY3_3 = f_3\ H(-w)\ H(-u)$	0	0	0	f_3	
$CY3_4 = f_4\ H(u)$	f_4	0	f_4	0	
$CY3_5 = f_5$	f_5	f_5	f_5	f_5	
$CY3_6 = f_6\ H(-u)$	0	f_6	0	f_6	
$CY3_7 = f_7\ H(w)\ H(u)$	f_7	0	0	0	
$CY3_8 = f_8\ H(w)$	f_8	f_8	0	0	
$CY3_9 = f_9\ H(w)\ H(-u)$	0	f_9	0	0	(15)

where u and w are calculated at the location (i,j–1/2,k+1/2). $CY4_\ell$ (ℓ = 1, ... 9) is defined in a similar way.

Finally, for z-direction, we have

$$\langle w\rangle_5 = w_{i,j,k} = [0, \langle w\rangle_5]\ (CZ5_1\ w_{145} + CZ5_2\ w_{45} + CZ5_3\ w_{245} +$$

$$+ CZ5_4\ w_{15} + CZ5_5\ w_5 + CZ5_6\ w_{25} +$$

$$+ CZ5_7\ w_{135} + CZ5_8\ w_{35} + CZ5_9\ w_{235}) -$$

$$- [0, -\langle w\rangle_5]\ (CZ5_1\ w_{14} + CZ5_2\ w_4 + CZ5_3\ w_{24} +$$

$$+ CZ5_4\ w_1 + CZ5_5\ w_0 + CZ5_6\ w_2 +$$

$$+ CZ5_7\ w_{13} + CZ5_8\ w_3 + CZ5_9\ w_{23}) . \qquad (16)$$

$$\langle w\rangle_6 = w_{i,j,k+1} = [0, \langle w\rangle_6]\ (CZ6_1\ w_{14} + CZ6_2\ w_4 + CZ6_3\ w_{24} +$$

$$+ CZ6_4\, w_1 + CZ6_5\, w_0 + CZ6_6\, w_2 +$$

$$+ CZ6_7\, w_{13} + CZ6_8\, w_3 + CZ6_9\, w_{23}) -$$

$$- [0.\ -\langle w\rangle_6]\,(CZ6_1\, w_{146} + CZ6_2\, w_{46} + CZ6_3\, w_{246} +$$

$$+ CZ6_4\, w_{16} + CZ6_5\, w_6 + CZ6_6\, w_{26} +$$

$$+ CZ6_7\, w_{136} + CZ6_8\, w_{36} + CZ6_9\, w_{236})\ . \qquad (17)$$

The coefficients $CZ5_\ell$ are

	$v_5 > 0,\ u_5 > 0$	$v_5 > 0,\ u_5 < 0$	$v_5 < 0,\ u_5 > 0$	$v_5 > 0,\ u_5 < 0$	
$CZ5_1 = f_1\ H(-v)\ H(u)$	0	0	f_1	0	
$CZ5_2 = f_2\ H(-v)$	0	C	f_2	f_2	
$CZ5_3 = f_3\ H(-v)\ H(-u)$	0	0	0	f_3	
$CZ5_4 = f_4\ H(u)$	f_4	0	f_4	0	
$CZ5_5 = f_5$	f_5	f_5	f_5	f_5	
$CZ5_6 = f_6\ H(-u)$	0	f_6	0	f_6	
$CZ5_7 = f_7\ H(v)\ H(u)$	f_7	0	0	0	
$CZ5_8 = f_8\ H(v)$	f_8	f_8	0	0	
$CZ5_9 = f_9\ H(v)\ H(-u)$	0	f_9	0	0	(18)

where u and v are evaluated at the location (i,j,k–1). Similar expressions can be written for $CX6_\ell$ (ℓ = 1, ... 9) with the u and v velocities evaluated at (i,j,k+1).

We introduce the following symbols for mass fluxes at the faces:

$$FX1 = (\rho uA)_{i-1/2,j,k+1/2}.$$

$$FX2 = (\rho uA)_{i+1/2,j,k+1/2}.$$

$$FY3 = (\rho vA)_{i,j-1/2,k+1/2}.$$

$$FY4 = (\rho vA)_{i,j+1/2,k+1/2}.$$

$$\overline{FZ}5 = (\rho wA)_{i,j,k}.$$

$$\overline{FZ}6 = (\rho wA)_{i,j,k+1}. \qquad (19)$$

where A denotes the cell surface area at corresponding locations. The convective term in Eq. 4, integrated over the z-momentum control volume by applying the Gauss theorem, can be expressed by

$$\int_{V_{f_0}} (\nabla \cdot \rho \tilde{v} w)\, dV = FX2\langle w\rangle_2 - FX1\langle w\rangle_1 + FY4\langle w\rangle_4$$

$$- FY3\langle w\rangle_3 + \overline{FZ}6\langle w\rangle_6 - \overline{FZ}5\langle w\rangle_5\ . \qquad (20)$$

Substituting in Eq. 18 the expressions for <w>1, <w>2, <w>3, <w>4, <w>5, and <w>6, given in Eqs. 11–14, 16, and 17, one obtains for the left side of Eq. 4:

$$
\begin{aligned}
\sum_{V_{f_0}} \frac{\partial}{\partial t}(\rho w)\,dV_f \;+\; & [0,FX2]\,\{CX2_1\,\dot{w}_{36} + CX2_2\,\dot{w}_6 + CX2_3\,\dot{w}_{46} \\
& + CX2_4\,\dot{w}_3 + CX2_5\,\dot{w}_0 + CX2_6\,\dot{w}_4 \\
& + CX2_7\,\dot{w}_{35} + CX2_8\,\dot{w}_5 + CX2_9\,\dot{w}_{45}\} - \\
-[0,-FX2]\,\{ & CX2_1\,\dot{w}_{236} + CX2_2\,\dot{w}_{26} + CX2_3\,\dot{w}_{246} \\
& + CX2_4\,\dot{w}_{23} + CX2_5\,\dot{w}_2 + CX2_6\,\dot{w}_{24} \\
& + CX2_7\,\dot{w}_{235} + CX2_8\,\dot{w}_{25} + CX2_9\,\dot{w}_{245}\} - \\
-[0,FX1]\,\{ & CX1_1\,\dot{w}_{136} + CX1_2\,\dot{w}_{16} + CX1_3\,\dot{w}_{146} \\
& + CX1_4\,\dot{w}_{13} + CX1_5\,\dot{w}_1 + CX1_6\,\dot{w}_{14} \\
& + CX1_7\,\dot{w}_{135} + CX1_8\,\dot{w}_{15} + CX1_9\,\dot{w}_{145}\} + \\
+[0,-FX1]\,\{ & CX1_1\,\dot{w}_{36} + CX1_2\,\dot{w}_6 + CX1_3\,\dot{w}_{46} \\
& + CX1_4\,\dot{w}_3 + CX1_5\,\dot{w}_0 + CX1_6\,\dot{w}_4 \\
& + CX1_7\,\dot{w}_{35} + CX1_8\,\dot{w}_5 + CX1_9\,\dot{w}_{45}\} + \\
+[0,FY4]\,\{ & CY4_1\,\dot{w}_{16} + CY4_2\,\dot{w}_6 + CY4_3\,\dot{w}_{26} \\
& + CY4_4\,\dot{w}_1 + CY4_5\,\dot{w}_0 + CY4_6\,\dot{w}_2 \\
& + CY4_7\,\dot{w}_{15} + CY4_8\,\dot{w}_5 + CY4_9\,\dot{w}_{25}\} - \\
-[0,-FY4]\,\{ & CY4_1\,\dot{w}_{146} + CY4_2\,\dot{w}_{46} + CY4_3\,\dot{w}_{246} \\
& + CY4_4\,\dot{w}_{14} + CY4_5\,\dot{w}_4 + CY4_6\,\dot{w}_{24} \\
& + CY4_7\,\dot{w}_{145} + CY4_8\,\dot{w}_{45} + CY4_9\,\dot{w}_{245}\} - \\
-[0,FY3]\,\{ & CY3_1\,\dot{w}_{136} + CY3_2\,\dot{w}_{36} + CY3_3\,\dot{w}_{236} \\
& + CY3_4\,\dot{w}_{13} + CY3_5\,\dot{w}_3 + CY3_6\,\dot{w}_{23} \\
& + CY3_7\,\dot{w}_{135} + CY3_8\,\dot{w}_{35} + CY3_9\,\dot{w}_{235}\} + \\
+[0,-FY3]\,\{ & CY3_1\,\dot{w}_{16} + CY3_2\,\dot{w}_6 + CY3_3\,\dot{w}_{26} \\
& + CY3_4\,\dot{w}_1 + CY3_5\,\dot{w}_0 + CY3_6\,\dot{w}_2 \\
& + CY3_7\,\dot{w}_{15} + CY3_8\,\dot{w}_5 + CY3_9\,\dot{w}_{25}\} + \\
+[0,\overline{FZ}6]\,\{ & CZ6_1\,\dot{w}_{14} + CZ6_2\,\dot{w}_4 + CZ6_3\,\dot{w}_{24} \\
& + CZ6_4\,\dot{w}_1 + CZ6_5\,\dot{w}_0 + CZ6_6\,\dot{w}_2 \\
& + CZ6_7\,\dot{w}_{13} + CZ6_8\,\dot{w}_3 + CZ6_9\,\dot{w}_{23}\} -
\end{aligned}
$$

$$
\begin{aligned}
&-\left[0.-\overline{FZ6}\right]\left\{CZ6_1\,w^{\bullet}_{146} + CZ6_2\,w^{\bullet}_{46} + CZ6_3\,w^{\bullet}_{246}\right.\\
&\qquad + CZ6_4\,w^{\bullet}_{16} + CZ6_5\,w^{\bullet}_{6} + CZ6_6\,w^{\bullet}_{26}\\
&\qquad \left. + CZ6_7\,w^{\bullet}_{136} + CZ6_8\,w^{\bullet}_{36} + CZ6_9\,w^{\bullet}_{236}\right\} -\\
&-\left[0.\,\overline{FZ5}\right]\left\{CZ5_1\,w^{\bullet}_{145} + CZ5_2\,w^{\bullet}_{45} + CZ5_3\,w^{\bullet}_{245}\right.\\
&\qquad + CZ5_4\,w^{\bullet}_{15} + CZ5_5\,w^{\bullet}_{5} + CZ5_6\,w^{\bullet}_{25}\\
&\qquad \left. + CZ5_7\,w^{\bullet}_{135} + CZ5_8\,w^{\bullet}_{35} + CZ5_9\,w^{\bullet}_{235}\right\} +\\
&+\left[0.-\overline{FZ5}\right]\left\{CZ5_1\,w^{\bullet}_{14} + CZ5_2\,w^{\bullet}_{4} + CZ5_3\,w^{\bullet}_{24}\right.\\
&\qquad + CZ5_4\,w^{\bullet}_{1} + CZ5_5\,w^{\bullet}_{0} + CZ5_6\,w^{\bullet}_{2}\\
&\qquad \left. + CZ5_7\,w^{\bullet}_{13} + CZ5_8\,w^{\bullet}_{3} + CZ5_9\,w^{\bullet}_{23}\right\}, \qquad (21)
\end{aligned}
$$

where the donor flow velocities are given by

$$w^{\bullet}_0 = Fz_0 \frac{\Delta z_0}{\overline{V}_0 \rho_0}, \qquad Fz_0 = (\rho wA)_{i,j,k+1/2}$$

$$w^{\bullet}_1 = Fz_1 \left(\frac{\Delta z_0}{\overline{V}_1 \rho_1} + \frac{\Delta z_6}{\overline{V}_6 \rho_6} \right) \Big/ 2, \qquad Fz_1 = (\rho wA)_{i-1,j,k+1/2}$$

$$w^{\bullet}_2 = Fz_2 \left(\frac{\Delta z_0}{\overline{V}_2 \rho_2} + \frac{\Delta z_6}{\overline{V}_{26} \rho_{26}} \right) \Big/ 2, \qquad Fz_2 = (\rho wA)_{i+1,j,k+1/2}$$

$$w^{\bullet}_3 = Fz_3 \left(\frac{\Delta z_0}{\overline{V}_3 \rho_3} + \frac{\Delta z_6}{\overline{V}_{36} \rho_{36}} \right) \Big/ 2, \qquad Fz_3 = (\rho wA)_{i,j-1,k+1/2}$$

$$w^{\bullet}_4 = Fz_4 \left(\frac{\Delta z_0}{\overline{V}_4 \rho_4} + \frac{\Delta z_6}{\overline{V}_{46} \rho_{46}} \right) \Big/ 2, \qquad Fz_4 = (\rho wA)_{i,j+1,k+1/2}$$

$$w^{\bullet}_5 = Fz_5 \frac{\Delta z_0}{\overline{V}_0 \rho_0}, \qquad Fz_5 = (\rho wA)_{i,j,k-1/2}$$

$$w^{\bullet}_6 = Fz_6 \frac{\Delta z_6}{\overline{V}_6 \rho_6}, \qquad Fz_6 = (\rho wA)_{i,j,k+3/2}$$

$$w^{\bullet}_{15} = Fz_{15} \frac{\Delta z_0}{\overline{V}_1 \rho_1}, \qquad Fz_{15} = (\rho wA)_{i-1,j,k-1/2}$$

$$w^{\bullet}_{25} = Fz_{25} \frac{\Delta z_0}{\overline{V}_2 \rho_2}, \qquad Fz_{25} = (\rho wA)_{i+1,j,k-1/2}$$

$$w^{\bullet}_{16} = Fz_{16} \frac{\Delta z_6}{\overline{V}_{16} \rho_{16}}, \qquad Fz_{16} = (\rho wA)_{i-1,j,k+3/2}$$

$$\dot{w}_{26} = Fz_{26}\frac{\Delta z_6}{\bar{\bar{V}}_{26}\rho_{26}}, \qquad Fz_{26} = (\rho wA)_{i-1,j,k+3/2}$$

$$\dot{w}_{35} = Fz_{35}\frac{\Delta z_0}{\bar{\bar{V}}_{3}\rho_{3}}, \qquad Fz_{35} = (\rho wA)_{i,j-1,k-1/2}$$

$$\dot{w}_{45} = Fz_{45}\frac{\Delta z_0}{\bar{\bar{V}}_{4}\rho_{4}}, \qquad Fz_{45} = (\rho wA)_{i,j+1,k-1/2}$$

$$\dot{w}_{36} = Fz_{36}\frac{\Delta z_6}{\bar{\bar{V}}_{36}\rho_{36}}, \qquad Fz_{36} = (\rho wA)_{i,j-1,k+1/2}$$

$$\dot{w}_{46} = Fz_{46}\frac{\Delta z_6}{\bar{\bar{V}}_{46}\rho_{46}}, \qquad Fz_{46} = (\rho wA)_{i,j+1,k+1/2}$$

$$\dot{w}_{13} = Fz_{13}\left(\frac{\Delta z_0}{\bar{\bar{V}}_{13}\rho_{13}} + \frac{\Delta z_6}{\bar{\bar{V}}_{136}\rho_{136}}\right)\Big/2, \qquad Fz_{13} = (\rho wA)_{i-1,j-1,k+1/2}$$

$$\dot{w}_{23} = Fz_{23}\left(\frac{\Delta z_0}{\bar{\bar{V}}_{23}\rho_{23}} + \frac{\Delta z_6}{\bar{\bar{V}}_{236}\rho_{236}}\right)\Big/2, \qquad Fz_{23} = (\rho wA)_{i+1,j-1,k+1/2}$$

$$\dot{w}_{14} = Fz_{14}\left(\frac{\Delta z_0}{\bar{\bar{V}}_{14}\rho_{14}} + \frac{\Delta z_6}{\bar{\bar{V}}_{146}\rho_{146}}\right)\Big/2, \qquad Fz_{14} = (\rho wA)_{i-1,j+1,k+1/2}$$

$$\dot{w}_{24} = Fz_{24}\left(\frac{\Delta z_0}{\bar{\bar{V}}_{24}\rho_{24}} + \frac{\Delta z_6}{\bar{\bar{V}}_{246}\rho_{246}}\right)\Big/2, \qquad Fz_{24} = (\rho wA)_{i+1,j+1,k+1/2}$$

$$\dot{w}_{135} = Fz_{135}\frac{\Delta z_0}{\bar{\bar{V}}_{13}\rho_{13}}, \qquad Fz_{135} = (\rho wA)_{i-1,j-1,k-1/2}$$

$$\dot{w}_{145} = Fz_{145}\frac{\Delta z_0}{\bar{\bar{V}}_{14}\rho_{14}}, \qquad Fz_{145} = (\rho wA)_{i-1,j+1,k-1/2}$$

$$\dot{w}_{235} = Fz_{235}\frac{\Delta z_0}{\bar{\bar{V}}_{23}\rho_{23}}, \qquad Fz_{235} = (\rho wA)_{i+1,j-1,k-1/2}$$

$$\dot{w}_{245} = Fz_{245}\frac{\Delta z_0}{\bar{\bar{V}}_{24}\rho_{24}}, \qquad Fz_{245} = (\rho wA)_{i+1,j+1,k-1/2}$$

$$\dot{w}_{136} = Fz_{136}\frac{\Delta z_6}{\bar{\bar{V}}_{136}\rho_{136}}, \qquad Fz_{136} = (\rho wA)_{i-1,j-1,k+3/2}$$

$$\dot{w}_{146} = Fz_{146}\frac{\Delta z_6}{\bar{\bar{V}}_{146}\rho_{146}}, \qquad Fz_{146} = (\rho wA)_{i-1,j+1,k+3/2}$$

$$\dot{w}_{236} = Fz_{236}\frac{\Delta z_6}{\bar{V}_{236}\rho_{236}}, \qquad Fz_{236} = (\rho wA)_{i+1,j-1,k+3/2}$$

$$\dot{w}_{246} = Fz_{246}\frac{\Delta z_6}{\bar{V}_{246}\rho_{246}}, \qquad Fz_{246} = (\rho wA)_{i+1,j+1,k+3/2}. \tag{22}$$

$\bar{V}m$ are cell volumes surrounding node m, and ρ is the upwinded density at corresponding locations.

The viscous terms in Eq. 4 are treated in the same way as before (Ref. 8), and the RHS of Eq. 4 can be written as

$$RHS = \bar{D}_6(w_6 - w_0) - \bar{D}_5(w_0 - w_5) + \bar{D}_4(w_4 - w_0) + \bar{D}_3(w_0 - w_3)$$

$$+ \bar{D}_2(w_2 - w_0) - \bar{D}_1(w_0 - w_1) + \int_{V_{f_0}}\left(S_w - \frac{\partial p}{\partial z}\right)dV . \tag{23}$$

The transient term is also treated in the same way as in Ref. 8, namely,

$$\int_{V_{f_0}}\frac{\partial}{\partial t}(\rho w)d\bar{V} \approx \frac{1}{2\Delta t}Az_0(\Delta z_0 + \Delta z_6)\left[\left(<\rho>_0^6 w\right)^{n+1} - \left(<\rho>_0^6 w\right)^n\right]. \tag{24}$$

The locations where the convective fluxes are defined are shown in Fig. 2.

Assembling all terms of Eq. 4, we have a finite-difference form of the z-momentum equation

$$a_0^{(1)} w_0^{n+1} = \sum_{i=1}^{26} a_{SUD_i}\dot{w}_i^{n+1} + \sum_{i=1}^{6} D_i w_i^{n+1} + b_0 - d_w(p_6 - p_0), \tag{25}$$

where

$$a_0^{(1)} = \frac{1}{2\Delta t}(\Delta z_0 + \Delta z_6)Az_0\left(<\rho>_0^6\right)^{n+1} - <S_w>\bar{V}_f +$$

$$+ <\rho>_0^6\frac{Az_0\Delta z_0}{\bar{V}_0\rho_0}\left(\frac{1}{2}[0,FX_0]CX2_5 + \frac{1}{2}[0,FY_0]CY4_5 + \frac{1}{2}[0,-FX_1]CX1_5 +\right.$$

$$\left. + \frac{1}{2}[0,-FY_3]CY3_5 + [0,-\bar{F}Z_5]CZ5_5\right) +$$

$$+ <\rho>_0^6\frac{Az_0\Delta z_6}{\bar{V}_6\rho_6}\left(\frac{1}{2}[0,FX_6]CX2_5 + \frac{1}{2}[0,FY_6]CY4_5 + \frac{1}{2}[0,-FX_{16}]CX1_5\right.$$

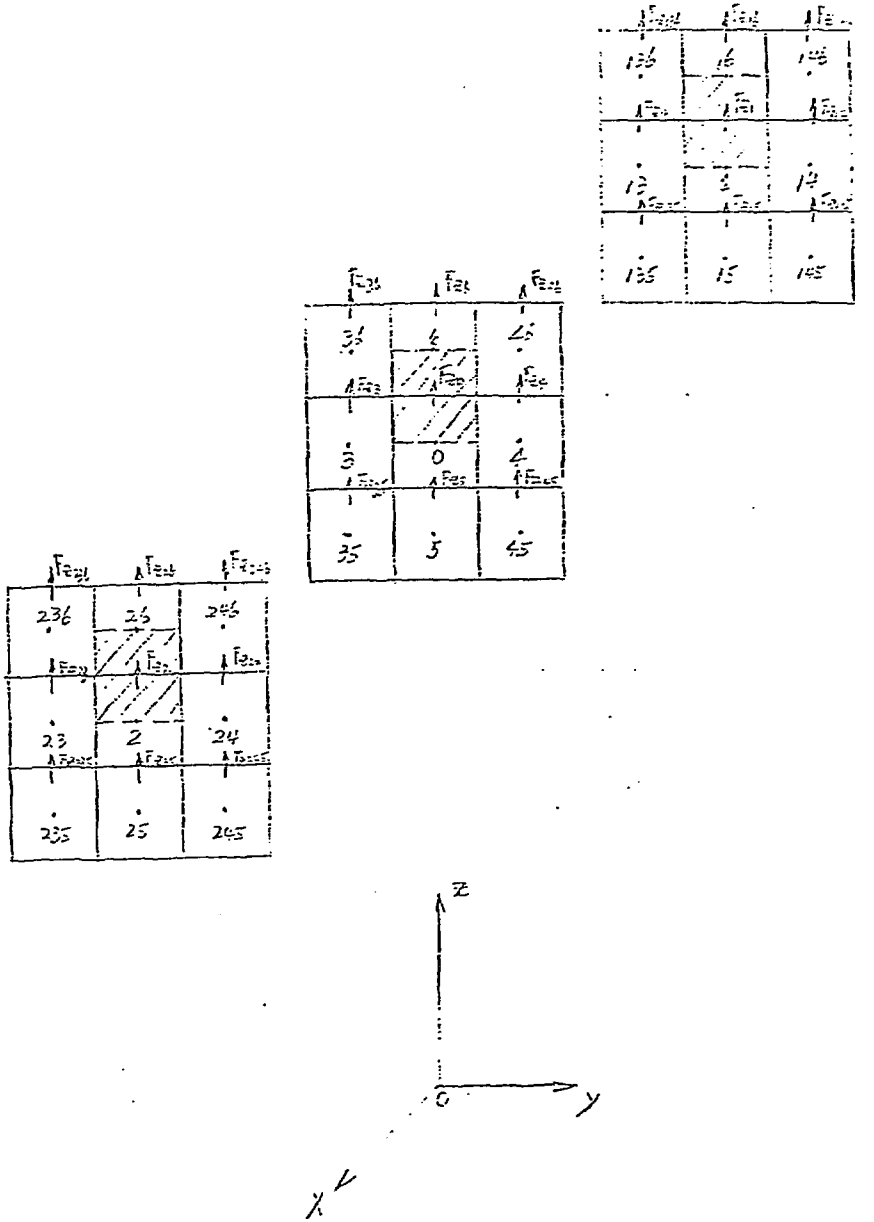

Fig. 2. Locations where convective fluxes for the z-momentum control volume are defined

$$+ \frac{1}{2}[0,-FY_{36}]CY3_5 + [0,\bar{F}Z_6]CZ6_5\Big) +$$
$$+ D_1 + D_2 + D_3 + D_4 + D_5 + D_6 \,. \tag{26}$$

with

$$FX_0 \equiv (\rho uA)_{i+1/2,j,k} = <\rho>_0^2 Ax_0u_0$$
$$FX_1 \equiv (\rho uA)_{i-1/2,j,k} = <\rho>_1^0 Ax_1u_1$$
$$FX_{16} \equiv (\rho uA)_{i-1/2,j,k+1} = <\rho>_6^{16} Ax_{16}u_{16}$$
$$FX_6 \equiv (\rho uA)_{i+1/2,j,k+1} = <\rho>_6^{26} Ax_6u_6$$
$$FY_3 \equiv (\rho vA)_{i,j-1/2,k} = <\rho>_3^0 Ay_3v_3$$
$$FY_0 \equiv (\rho vA)_{i,j+1/2,k} = <\rho>_0^4 Ay_0v_0$$
$$FY_{36} \equiv (\rho vA)_{i,j-1/2,k+1} = <\rho>_{63}^6 Ay_{63}v_{63}$$
$$FY_6 \equiv (\rho vA)_{i,j+1/2,k+1} = <\rho>_6^{64} Ay_6v_6$$
$$\bar{F}Z_5 \equiv (\rho wA)_{i,j,k} = <\rho>_0^5 Az_0w_0$$
$$\bar{F}Z_6 \equiv (\rho wA)_{i,j,k+1} = <\rho>_0^6 Az_0w_0 \tag{27}$$

and

$$b_0 = w_0^n\left[\frac{1}{2\Delta t}(\Delta z_0 + \Delta z_6)\, Az_0 <\rho>_0^6\right] + S_w V_{0_f} \tag{28}$$

$$d_w = 2V_{f_0}/(\Delta z_0 + \Delta z_6) = 2/\left(\Delta z_0/V_{f_0} + \Delta z_6/V_{f_6}\right). \tag{29}$$

In the above equations, D_i are diffusivities at cells i,

$<S_w>$ is the integrated source term,

$<\rho>_i^j$ is the upwind density depending on velocity between nodes i and j,

and a_{SUD_i} are the 26 coefficients for w* given by (we drop the subscript SUD):

$$a_1 = \{[0,-FX1]CX1_5 - [0,FY4]CY4_4 - [0,-FY3]CY3_4 - [0,\bar{F}Z6]CZ6_4 +$$
$$+ [0,-\bar{F}Z5]CZ5_4\} \,.$$

$$a_2 = \{[0,-FX2]CX2_5 - [0,FY4]CY4_6 - [0,-FY3]CY3_6 - [0,\bar{F}Z6]CZ6_6 + - [0,-\bar{F}Z5]CZ5_6\},$$

$$a_3 = \{-[0,FX2]CX2_4 - [0,-FX1]CX1_4 + [0,FY3]CY3_5 - [0,FZ6]CZ6_8 + - [0,-FZ5]CZ5_8\}.$$

$$a_4 = \{-[0,FX2]CX2_6 - [0,-FX1]CX1_6 + [0,-FY4]CY4_5 - [0,FZ6]CZ6_2 + - [0,-FZ5]CZ5_2\}.$$

$$a_5 = \{-[0,FX2]CX2_8 - [0,-FX1]CX1_8 - [0,FY4]CY4_8 - [0,-FY3]CY3_8 + + [0,FZ5]CZ5_5\}.$$

$$a_6 = \{-[0,FX2]CX2_2 - [0,-FX1]CX1_2 - [0,FY4]CY4_2 - [0,-FY3]CY3_2 + + [0,-FZ6]CZ6_5\}.$$

$$a_{13} = \{[0,FX1]CX1_4 + [0,FY3]CY3_4 - [0,\bar{F}Z6]CZ6_7 - [0,-\bar{F}Z5]CZ5_7\},$$

$$a_{15} = \{[0,FX1]CX1_8 - [0,FY4]CY4_7 - [0,-FY3]CY3_7 + [0,\bar{F}Z5]CZ5_4\}$$

$$a_{35} = \{-[0,FX2]CX2_7 - [0,-FX1]CX1_7 + [0,FY3]CY3_8 + [0,\bar{F}Z5]CZ5_8\},$$

$$a_{36} = \{-[0,FX2]CX2_1 - [0,-FX1]CX1_1 + [0,FY3]CY3_2 + [0,-\bar{F}Z6]CZ6_8\},$$

$$a_{24} = \{[0,-FX2]CX2_6 + [0,-FY4]CY4_6 - [0,\bar{F}Z6]CZ6_3 - [0,-\bar{F}Z5]CZ5_3\},$$

$$a_{26} = \{[0,-FX2]CX2_2 - [0,FY4]CY4_3 - [0,-FY3]CY3_3 + [0,-\bar{F}Z6]CZ6_6\},$$

$$a_{46} = \{-[0,FX2]CX2_3 - [0,-FX1]CX1_3 + [0,-FY4]CY4_2 + [0,-\bar{F}Z6]CZ6_2\},$$

$$a_{23} = \{[0,-FX2]CX2_4 + [0,FY3]CY3_6 - [0,-\bar{F}Z5]CZ5_9 - [0,\bar{F}Z6]CZ6_9\},$$

$$a_{14} = \{[0,FX1]CX1_6 + [0,-FY4]CY4_4 - [0,\bar{F}Z6]CZ6_1 - [0,-\bar{F}Z5]CZ5_1\},$$

$$a_{45} = \{-[0,FX2]CX2_9 - [0,-FX1]CX1_9 + [0,-FY4]CY4_8 + [0,\bar{F}Z5]CZ5_2\},$$

$$a_{16} = \{[0,FX1]CX1_2 - [0,FY4]CY4_1 - [0,-FY3]CY3_1 + [0,-\bar{F}Z6]CZ6_4\},$$

$$a_{25} = \{[0,-FX2]CX2_8 - [0,FY4]CY4_9 - [0,-FY3]CY3_9 + [0,\bar{F}Z5]CZ5_6\},$$

$$a_{135} = \{[0,FX1]CX1_7 + [0,FY3]CY3_7 + [0,\bar{F}Z5]CZ5_7\},$$

$$a_{136} = \{[0,FX1]CX1_1 + [0,FY3]CY3_1 + [0,-\bar{F}Z6]CZ6_7\},$$

$$a_{235} = \{[0,-FX2]CX2_7 + [0,FY3]CY3_9 + [0,\bar{F}Z5]CZ5_9\},$$

$$a_{236} = \{[0,-FX2]CX2_1 + [0,FY3]CY3_3 + [0,-\bar{F}Z6]CZ6_9\},$$

$$a_{145} = \{[0,FX1]CX1_9 + [0,-FY4]CY4_7 + [0,\bar{F}Z5]CZ5_1\}.$$

$$a_{146} = \left\{[0,FX1]CX1_3 + [0,-FY4]CY4_1 + \left[0,-\overline{F}Z6\right]CZ6_1\right\},$$

$$a_{245} = \left\{[0,-FX2]CX2_9 + [0,-FY4]CY4_9 + \left[0,\overline{F}Z5\right]CZ5_3\right\},$$

$$a_{246} = \left\{[0,-FX2]CX2_3 + [0,-FY4]CY4_3 + \left[0,-\overline{F}Z6\right]CZ6_3\right\}. \tag{30}$$

The nonconservative form of a_0 has been given in Eq. 26. A second form of a_0 is obtained by subtracting the continuity equation from the first form. In the z-momentum equation, this is given by

$$a_0^{(II)} = a_0^{(I)} - \frac{1}{2}(\text{mass eq. at cell 0}) - \frac{1}{2}(\text{mass eq. at cell 6}) =$$

$$= <\rho>_0^6 \frac{Az_0}{2\Delta t}\left(\frac{\rho_6^n}{\rho_6^{n+1}}\,\Delta z_6 + \frac{\rho_0^n}{\rho_0^{n+1}}\,\Delta z_0\right) +$$

$$+ <\rho>_0^6 \frac{Az_0\,\Delta z_6}{\overline{V}_{f_6}\rho_6}\left\{\frac{1}{2}[0,-FX6] + \frac{1}{2}[0,-FY6] + \frac{1}{2}[0,FX16] +\right.$$

$$\left. + \frac{1}{2}[0,FY36] + \left[0,-\overline{F}Z6\right] + FZ0\right\} +$$

$$+ <\rho>_0^6 \frac{Az_0\,\Delta z_0}{\overline{V}_{f_0}\rho_0}\left\{\frac{1}{2}[0,-FX0] + \frac{1}{2}[0,-FY0] + \frac{1}{2}[0,FX1] +\right.$$

$$\left. + \frac{1}{2}[0,FY3] + \left[0,\overline{F}Z5\right] - FZ0\right\} +$$

$$+ D_1 + D_2 + D_3 + D_4 + D_5 + D_6 -$$

$$- <\rho>_0^6 \frac{Az_0\,\Delta z_6}{\overline{V}_{f_6}\rho_6}\left\{\frac{1}{2}[0,FX6](1 - CX2_5) + \frac{1}{2}[0,FY6](1 - CY4_5) +\right.$$

$$\left. + \left[0,\overline{F}Z6\right](1 - CZ6_5)\right\} -$$

$$- <\rho>_0^6 \frac{Az_0\,\Delta z_0}{\overline{V}_{f_0}\rho_0}\left\{\frac{1}{2}[0,FX0](1 - CX2_5) + \frac{1}{2}[0,FY0](1 - CY4_5) +\right.$$

$$+ \frac{1}{2}[0,-FX1](1 - CX1_5) + \frac{1}{2}[0,-FY3](1 - CY3_5) +$$

$$\left. + \left[0,-\overline{F}Z5\right](1 - CZ6_5)\right\}. \tag{31}$$

The above formulations can be extended similarly to the x and y momentum equations.

2 Flow–Modulated Approach and Cos (theta) Approach

The approach explained in Sec. 1.2 is independent of the way of computing the weights (f's), hence the coefficients $CX1_\ell$, $CX2_\ell$, $CY3_\ell$, $CY4_\ell$, $CZ5_\ell$, and $CZ6_\ell$ in Eqs. 8, 15, and 18. In the code, we have two options for computing these weights and coefficients:

1. The Flow–Modulated (FM) approach explained in Ref. 8 for the case of the energy equation.

2. An approach based on the cosine of the angle between velocity vector and the coordinate direction corresponding to the scalar components of the momentum equation being treated. We refer to this second variant as the cos (theta), or CT, approach.

Because it is not clear at present whether one option is to be preferred to the other, both have been retained so far. They are briefly reviewed below.

2.1 Flow–Modulated Approach

The coefficients are computed by the following equations, reported for the sake of completeness from Ref. 8:

$$CX1_7 = CX1_2 = C_{xyz} = C(m_x,m_y,m_z) = \frac{1}{3}\min\left(1,\frac{m_y}{m_x},\frac{m_z}{m_x}\right) \tag{32}$$

$$CY4_7 = CY3_7 = C_{yzx} = \frac{1}{3}\min\left(1,\frac{m_z}{m_y},\frac{m_x}{m_y}\right) \tag{33}$$

$$CZ67 = CZ57 = C_{zxy} = \frac{1}{3}\min\left(1,\frac{m_x}{m_z},\frac{m_y}{m_z}\right) \tag{34}$$

$$CX2_4 = CX1_4 = S_{xyz} = S(m_x,m_y,m_z) = \frac{1}{2}\left\{\max\left[0,\min\left(1,\frac{m_y}{m_x}\right)-\frac{m_z}{m_x}\right]+\frac{1}{3}\min\left(1,\frac{m_y}{m_x},\frac{m_z}{m_x}\right)\right\} \tag{35}$$

$$CX2_8 = CX1_8 = S_{xzy} = S(m_x,m_z,m_y) = \frac{1}{2}\left\{\max\left[0,\min\left(1,\frac{m_z}{m_x}\right)-\frac{m_y}{m_x}\right]+\frac{1}{3}\min\left(1,\frac{m_y}{m_x},\frac{m_z}{m_x}\right)\right\} \tag{36}$$

$$CY4_4 = CY3_4 = S_{yxz} = \frac{1}{2}\left\{\max\left[0,\min\left(1,\frac{m_x}{m_y}\right)-\frac{m_z}{m_y}\right]+\frac{1}{3}\min\left(1,\frac{m_z}{m_y},\frac{m_x}{m_y}\right)\right\} \tag{37}$$

$$CZ6_4 = CZ5_4 = S_{zxy} = \frac{1}{2}\left\{\max\left[0,\min\left(1,\frac{m_x}{m_y}\right)-\frac{m_y}{m_z}\right]+\frac{1}{3}\min\left(1,\frac{m_x}{m_z},\frac{m_y}{m_z}\right)\right\} \tag{38}$$

$$CY4_8 = CY3_8 = S_{yzx} = \frac{1}{2}\left\{\max\left[0,\min\left(1,\frac{m_z}{m_y}\right)-\frac{m_x}{m_y}\right]+\frac{1}{3}\min\left(1,\frac{m_z}{m_y},\frac{m_x}{m_y}\right)\right\} \tag{39}$$

$$CZ6_8 = CZ5_8 = S_{zyx} = \frac{1}{2}\left\{\max\left[0,\min\left(1,\frac{m_y}{m_z}\right),-\frac{m_x}{m_z}\right]+\frac{1}{3}\min\left(1,\frac{m_y}{m_z},\frac{m_x}{m_z}\right)\right\} \tag{40}$$

In these equations, m represents mass flows. The analytical expressions for $CX1_7$ and $CX2_7$ (and similarly for the other couples of symbols) are identical, but the respective mass fluxes are obviously computed on opposite faces of the control volume.

2.2 Cos (theta) Approach

Let us consider the z component of the momentum equation, and let indices 1 to 6 label the boundary faces, according to the usual conventions. Let

$$\left|\vec{V}_i\right| = \left(u_i^2 + v_i^2 + w_i^2\right)^{1/2} \tag{41}$$

be the modulus of the velocity vector on face i, and

$$\begin{aligned} \tilde{u}_i &= |u_i|/\left|\vec{V}_i\right| \\ \tilde{v}_i &= |v_i|/\left|\vec{V}_i\right| \\ \tilde{w}_i &= |w_i|/\left|\vec{V}_i\right| \end{aligned} \tag{42}$$

be the absolute values of the normalized velocity components on face i. Unlike the case of the energy equation, where control volumes are centered and velocities are defined on the bounding faces, in this case control volumes are staggered and the velocity components u_i, v_i, and w_i are not available at the center point of the respective faces. Therefore, interpolations between available values on the centered faces are required. The same holds for the calculation of the mass fluxes needed in Eqs. 32–40.

Let θ_1, θ_2 be the angles between velocity vectors $\vec{v}_1$, $\vec{v}_2$, and the x axis, θ_3, θ_4 between $\vec{v}_3$, $\vec{v}_4$ and the y axis; θ_5, θ_6 between $\vec{v}_5$, $\vec{v}_6$ and the z axis. The weighting factors are then computed on face 1 by:

$$f_5 = (\cos\theta_1)^2$$

$$f_1 = f_3 = f_7 = f_9 = (1 - f_5)\frac{\tilde{v}_1\tilde{w}_1}{\tilde{v}_1^n + \tilde{w}_1^n + \tilde{v}_1\tilde{w}_1}$$

$$f_2 = f_8 = (1 - f_5)\frac{\tilde{w}_1^n}{\tilde{v}_1^n + \tilde{w}_1^n + \tilde{v}_1\tilde{w}_1}$$

$$f_4 = f_6 = (1 - f_5)\frac{\tilde{v}_1^n}{\tilde{v}_1^n + \tilde{w}_1^n + \tilde{v}_1\tilde{w}_1} \tag{43}$$

with n = 1 as default. Similar equations, obtained by rotating velocity components, apply to the faces normal to the y and z coordinate directions.

A FORTRAN statement such as

$$f_5 = \max [f_5, \cos (\text{lim})] \tag{44}$$

allows to set a minimum value for the central weights f_5 and therefore for the central coefficients $CX1_5$, $CX2_5$, $CY3_5$, $CY4_5$, $CZ5_5$, and $CZ6_5$. Setting cos (lim) = 1, hence, $f_5 = 1$, $f_i = 0$ (i = 1, .. 4; 6, ..9), one has the subcase of a pure upwind calculation, because it can be verified easily on the equations of Sec. 1.2. This has also been checked numerically. Default is cos (lim) = 0, although it seems that in some cases better results can be obtained by setting cos (lim) = 0.5 (see test case III in Sec. 4).

3 Treatment of Boundary Conditions

The treatment of boundary conditions is particularly difficult because of the staggered meshes and the large number of neighboring cells that must be considered. This topic has not been sufficiently investigated so far. We distinguish between the following cases:

1) Interpolation of Velocities (or Mass Flows) for Boundary Cells. As explained in Sec. 4.4, this interpolation is necessary to calculate velocities or mass flows at the centerpoint of the faces of staggered cells. When a value to be interpolated lies out of the boundary, the boundary value is taken from array VELBN (or FLOWB).

2) Calculation of Starred Velocities. Starred velocities up to index 6 (u_1^* to u_6^*, v_1^* to v_6^*, and w_1^* to w_6^*) are computed as usual in COMMIX-1C (Ref. 8), taking into account the boundary conditions. For the other starred velocities, either the values in existing cells are used or (if these cells do not exist in the computational domain) values for cell o are used. The use of boundary conditions in cells with an index beyond 6 destroys the accuracy of the scheme. The reason for this has not been so far investigated.

4 Numerical Verification

Both options explained in Sec. 2 (the FM and the CT approaches) have been tested, in comparison with results from the pure-upwind discretization scheme, in the following cases:

I Natural convection of air in a square pipe.

II Two-dimensional jet. The jet enters a square domain with solid walls at a corner at 45° (along the diagonal). An outlet is at the opposite corner.

III Three-dimensional jet. As above, in a three-dimensional domain.

IV (Two-dimensional) Impinging of two streams with the same velocity and different temperatures. The streams enter a square domain from two adjacent edges and impinge along the diagonal.

V (Two-dimensional) Impinging of two streams with different velocities and temperatures.

Plots referring to these five test cases are labeled according to the code below. A label NXXn is given where:

N is the roman number referring to the test case.

XX is UP for upwind calculation.
FM for SUD calculation with the FM option.
CT for SUD calculation with the CT option.

n is a small letter given the order within the NXX group.

In the following, we briefly characterize the single test cases and explain the main results obtained.

I Natural Convection of Air in a Square Pipe

The driving temperature difference is $\Delta T = 10°K$ and the Rayleigh number is 10^3.

Plots IUPa and IUPb show the temperature and velocity distributions obtained with the upwind discretization scheme both for energy and momentum equations.

Plot IFMa/b shows the same distributions as above obtained with the FM approach. Results obtained with the CT approach are almost identical with those of the FM method. These calculations have been made for checking purposes and the results are very close to those of the upwind scheme, because in this test problem both temperature and velocity fields display relatively smooth gradients and therefore the numerical diffusion is small.

All of these calculations were run up to convergence to a steady state.

II Two-Dimensional Jet

A jet enters a square domain from the lower left corner with velocity $\bar{v} = \sqrt{2}$ (two velocity components equal to 1). Without molecular and numerical diffusion, the jet is expected to travel along the diagonal to the opposite corner without losing speed.

Plot IIUPa shows the velocity distribution computed with the upwind scheme. The jet looses its identity after a few meshes from the inlet. Calculation refers to the (xy) plane.

Plot IIFMa shows the velocity distribution obtained with the FMSUD scheme. The jet preserves its identity up to the opposite corner, though losing much of its strength.

Plot IICTa shows the velocity distributions obtained with the CT option. The jet preserves its full intensity up to the next corner.

Calculations performed with either the FM or the CT approach failed to converge and were stopped after 60 time steps. Continuing the calculations beyond some time point spoils the results and finally leads to loss of the jet identity. The reasons for this behavior are not yet understood.

III Three-Dimensional Jet

A jet enters a cubic domain from a corner with velocity $\bar{v} = \sqrt{3}$ (three velocity components equal to 1). Without molecular and numerical diffusion, the jet travels along the diagonal to the opposite corner without losing speed. Numerical results obtained for the velocity along the diagonal are shown in Table 1.

Even the best results obtained with the CTSUD (n = 1) option (third column from left in the above table) show a loss of about 2/3 of the jet intensity. Comparison between the third and fourth columns of the table shows that the parameter n has an enormous impact. The parameter n affects the weight of the corner cell in comparison with the weights of the side cells (for instance, it affects the coefficient $CS1_7$, compared to $CX1_4$ and $CX1_8$, under the constraint $CX1_4 + CX1_8 + CX1_7 = 1 - f_5 = 1 - CX1_5$. Increasing n, the weight of corner cells increases. One must therefore conclude that the inaccuracy of the results obtained so far depends very probably on a wrong weight distribution between corner and side cells. Substantiation of this suspicion would require a parametric analysis of numerical results which has not been undertaken so far for time reasons.

IV Impinging of Two Streams with Same Velocity and Different Temperatures

The streams enter a square domain from two adjacent edges and impinge along the diagonal. In the absence of molecular and numerical diffusion, the isotherms are expected to concentrate on the diagonal. The spreading of the isotherms off the diagonal is a measure of the numerical diffusion of the scheme used.

Plots IVUPa and IVUPb show the temperature distribution and velocity field in the case of an upwind calculation. The temperatures of the inlet flows were 50°C and 150°C, respectively. Numerical diffusion in this case is very large.

Plot IVFMa shows results of a calculation made with the FM option in the energy equation alone (ISKEW = 1), not in the momentum equation. Numerical diffusion of enthalpy is well suppressed. The velocity field did not change with respect to the upwind calculation, because the density was considered to be independent of pressure and temperature.

Plot IVCTa shows the temperature distribution obtained with the CT option in the momentum equation. Apart from converging slightly faster in number of time-steps (55 against 63), the temperature distribution is essentially the same as before. This is an obvious result because the two streams have the same velocities and therefore there is no numerical diffusion of momentum.

Table 1. Three-dimensional jet problem: velocity along the diagonal

$\bar{v}$	Upwind	FMSUD	CTSUD with n = 1 in Eq. 43	CTSUD with n = 2 in Eq. 43
i = j = k = 2	0.21	0.64	1.07	1.45
3	0.09	0.40	1.13	1.03
4	0.07	0.34	1.01	0.90
5	0.07	0.35	0.95	0.79
6	0.08	0.25	0.95	0.75
7	0.08	0.26	0.92	0.67
8	0.08	0.27	0.89	0.75
9	0.09	0.24	0.85	0.52
10	0.09	0.27	0.81	0.63
11	0.08	0.25	0.77	0.34
12	0.07	0.18	0.73	0.44
13	0.09	0.14	0.69	0.09
14	0.21	0.28	0.66	0.41

All test cases were run up to convergence.

V Impinging of Two Streams with Different Velocities and Temperatures

The geometry is the same as in the above case, but now the two streams have velocities : $_B$ = 0.15 *m/s* and v_B – 0.1 *m/s*. Thus, they impinge along a line inclined by the angle θ = arc cos (2/3) with respect to the x–axis.

Plots VUPa and VUPb show temperature and velocity distributions in case of an upwind calculation. The numerical diffusion is very large.

Plots VUPc and VUPd show results obtained with the FMSUD scheme in the energy equation but not in the momentum equation. The results are considerably improved with respect to the previous case, but the isotherms are displaced upward with respect to the line where the streams impinge.

Plots VFMa, VFMb, VCTa, and VCTb show the same calculation made with the FM and CT option, respectively. In both cases, the results display a bending of the flow field below the line along which the two streams are expected to impinge. This can be interpreted as the consequence of an incorrect distribution of weights between center and side cells. This suspicion is substantiated by the results shown in the next two plots.

Plots VCTc and VCTd show results obtained using cos lim = 0.5 in Eq. 43, instead of the default cos lim = 0. This implies that the central cell must retain at least half of the total weight. The results are better than in the previous case and show that the weight distribution among the cells is both important and difficult to evaluate properly.

All test cases were run up to convergence.

5 Conclusions

5.1 Accuracy of Numerical Results

The evaluation of the test cases discussed in Sec. 4 shows that results obtained with both FMSUD and CTSUD are generally more accurate than results obtained with the upwind scheme.

5.2 Convergence Behavior

When convergence is achieved with the SUD scheme, this occurs in a number of time-steps comparable to (sometime faster than) that for the upwind scheme. The computational time is, however, larger due to additional computation necessary to evaluate the coefficients of the 26 adjacent cells. For small problems, this can account for up to 50% more CPU time; for larger problems with more than a few thousand cells, where most of the CPU time is spent in the Poisson solver, the additional effort is probably about 10 to 15%.

Problems arise in some cases, as in the jet problem, when convergence is not achieved and results deteriorate with increasing number of time-steps, beyond some threshold. The reasons for this behavior have not been investigated.

5.3 Choice of Weights

Numerical results show that the SUD method is very sensitive to the choice of weight distribution among central, side, and corner cells. This is shown especially by the preliminary results obtained in the three-dimensional jet problems. This difficulty is less serious in two-dimensional problem where corner cells do not exist.

Tackling this problem would require additional work, from both the analytical and numerical standpoints. Sensitive analysis with respect to parameter variations would be required.

5.4 Implementation of the Method and Treatment of the Boundary Conditions

Implementation of the SUD scheme into the treatment of the momentum equation of an existing computer code is very demanding, especially in the case of staggered meshes, because of the large number of side and corner cells (26) that must be considered. For the same reason, the treatment of boundary conditions is very complicated. It is thought to be correct for the test cases discussed in this report, but caution should be used when

applying the method to other test cases with different boundary conditions. This topic would therefore need further analysis.

As a comparison, the QUICK method of Ref. 14 requires the treatment of only 12 side cells and allows a relatively simpler treatment of boundary conditions.

5.5 General Evaluation

A definite assessment of the SUD scheme is not possible at this moment, nor is a comparison with the above-mentioned QUICK method been attempted thus far.

It is our opinion that the SUD scheme has the potential to become a practicable alternative to high-order schemes. The exploitation of this potentiality requires, however, additional analytical and numerical work.

Acknowledgment

Best thanks are due to Mrs. S. Moll for her enduring and excellent work in typing the manuscript.

References

1. B. P. Leonard, *A Survey of Finite Differences with Upwinding for Numerical Modeling of the Incompressible Convection Diffusion Equation*, Computational Techniques in Transient and Turbulent Flow, C. Taylor and K. Morgan, eds., Pineridge Press (1981).

2. J. von Neumann and R. D. Richtmyer, *A Method for the Numerical Calculations of Hydrodynamical Shocks*, J. App. Phys *21* (1950).

3. G. D. Raithby, *Skew Upstream Differencing Schemes for Problems Involving Fluid Flow*, Comp. Meth. Appl. Mech. Eng., *9*, 153-164 (1976).

4. M. A. Leschziner, *Practical Evaluation of Three Finite Difference Schemes for the Computation of Steady-State Recirculating Flows*, Comp. Meth. Appl. Mech. Eng., *23*, 293-312 (1980).

5. Y. A. Hassan, J. B. Rice, and J. H. Kim, *Cause and Cure of Stability Problems in the Skew Upwind Differencing Scheme*, Trans. ANS, *45* (1983).

6. Y. A. Hassan, *Implementation of a Mass-Flow-Weighted Skew-Upwind Differencing Scheme in COMMIX-1A*, Electric Power Research Institute Report EPRI NP-3518 (1984).

7. *COMMIX-1B: A Three-Dimensional Transient Single-Phase Computer Program for Thermal Hydraulic Analysis of Single and Multicomponent Systems, Vol. I, Equations and Numerics; Vol. II, User's Manual*, NUREG/CR-4348, Argonne National Laboratory Report ANL-85-42 (Sept. 1985).

8. *COMMIX-1C: A Three-Dimensional Transient Single-Phase Computer Program for Thermal Hydraulic Analysis of Single and Multicomponent Systems, Vol. I, Equations and Numerics; Vol. II, User's Manual*, NUREG/CR-5649, Argonne National Laboratory Report ANL-90-33 (Nov. 1990).

9. M. Chapman, *FRAM Nonlinear Damping Algorithms for the Continuity Equation*, J. Comp. Phys. 44, 84-103 (1981).

10. W. C. Rivard, O. A. Farmer, T. D. Butler, and P. J. O'Rourke, *A Method for Increased Accuracy in Eulerian Fluid Dynamics Calculations*, Los Alamos National Laboratory Report LA-5426-MS (1973).

11. J. P. Boris and D. L. Book, *Solution of Continuity Equations by the Method of Flux Corrected Transport*, in Vol. 16 of Methods in Computational Physics (eds, B. Alder, S. Fernbach, and M. Rotenberg), Academic Press (1976).

12. H. Takewaki, A. Nishiguchi, and T. Yabe, *Cubic Interpolated Pseudo-Particle Method (CIP) for Solving Hyperbolic-Type Equations*, J. Comp. Phys., *61*, 261-268 (1985).

13. T. Yabe and H. Takewaki, *CIP: A New Numerical Solver for General Nonlinear Hyperbolic Equations in Multi-dimension*, KfK-4154 (1986).

14. B. P. Leonard, *A Stable and Accurate Convective Modeling Procedure Based on Quadratic Upstream Interpolation*, in Comp. Meth. in App. Mech. & Engrg., *19*, 59-98 (1978).

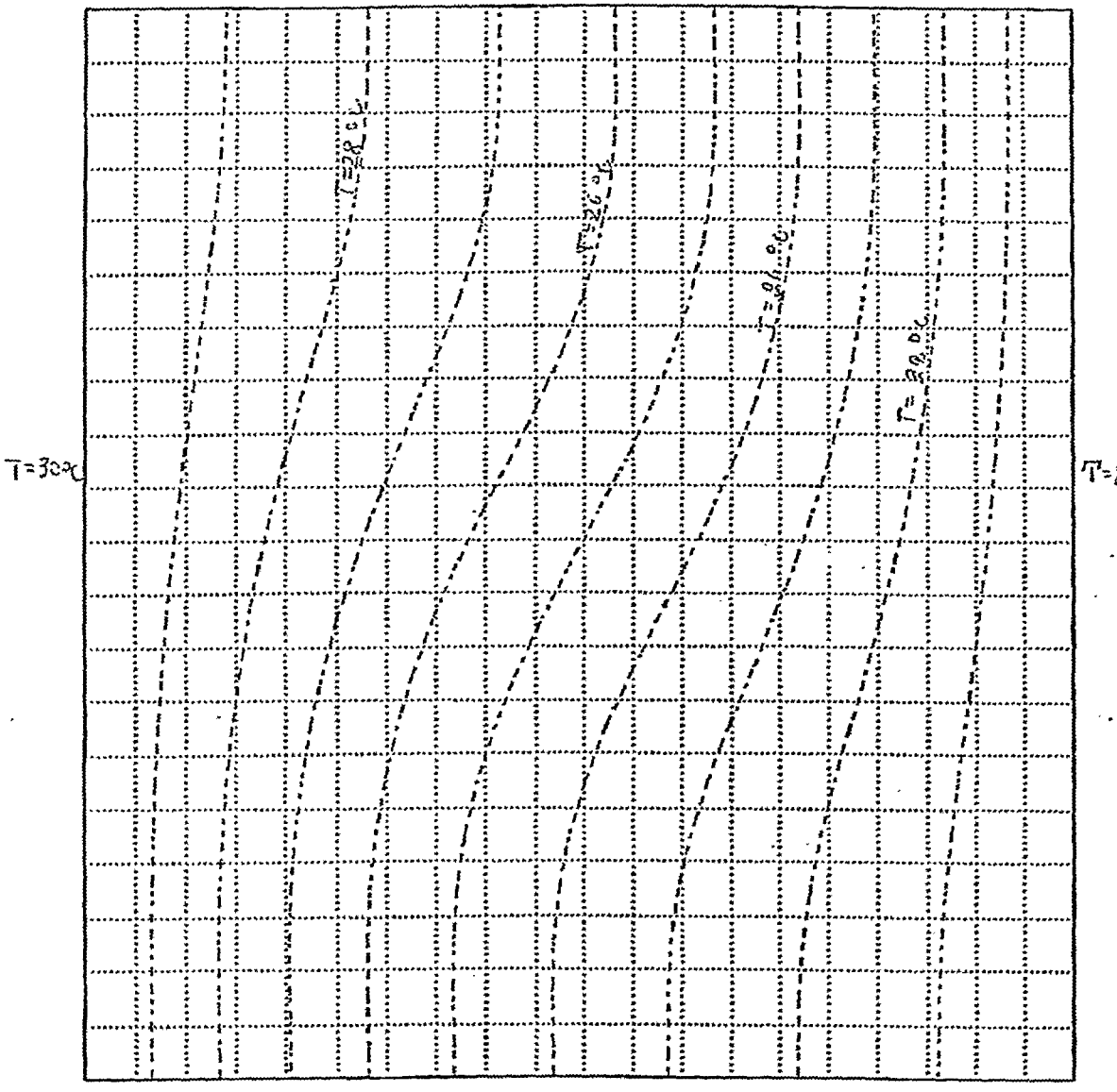

K = 1
Time: $2.41*10^3$ s

Case I: Plot UPa

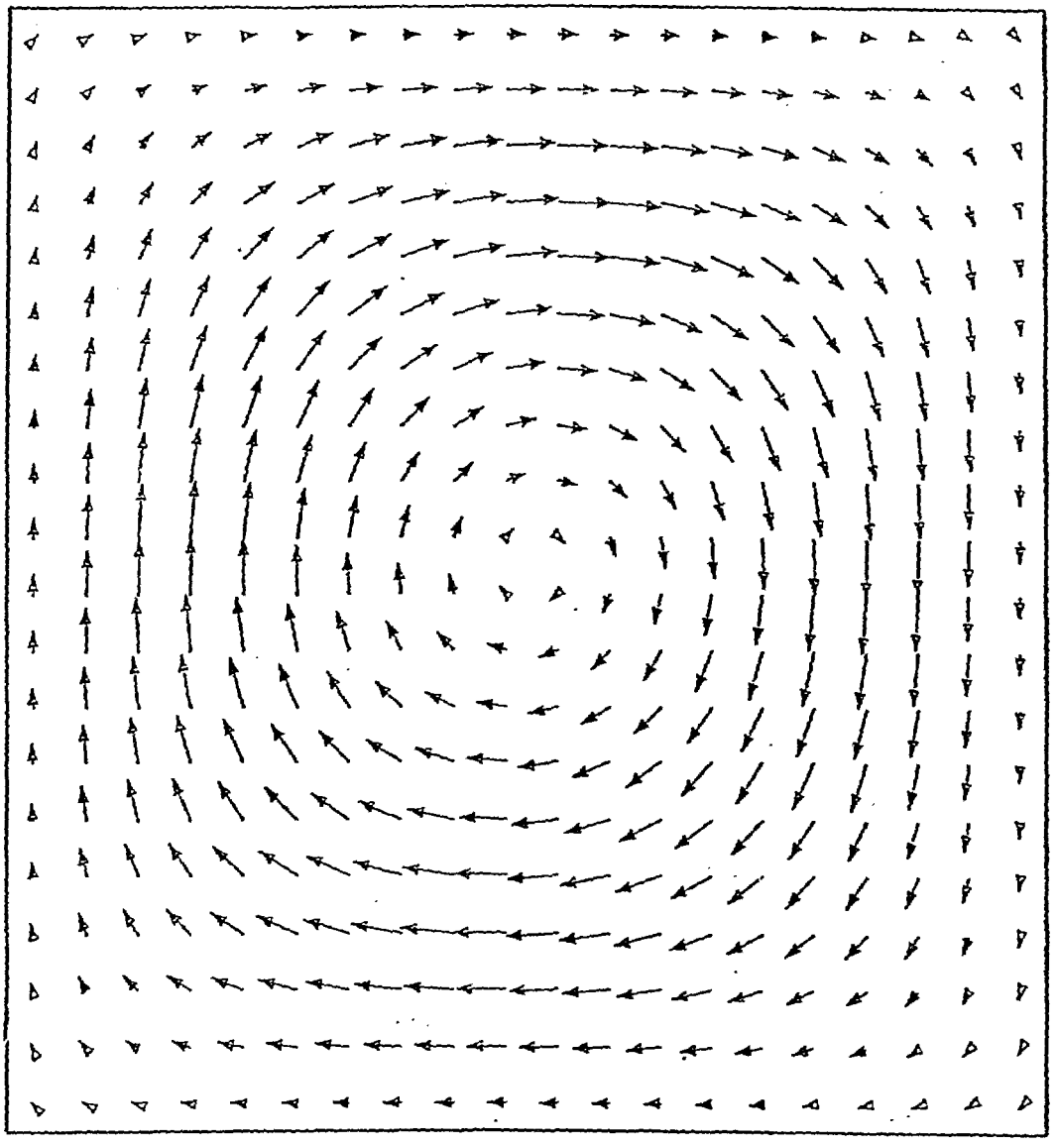

K = 1

$2.33*10^{-2}$ m/s

Time: $2.41*10^{3}$ s

Case I: Plot UPb

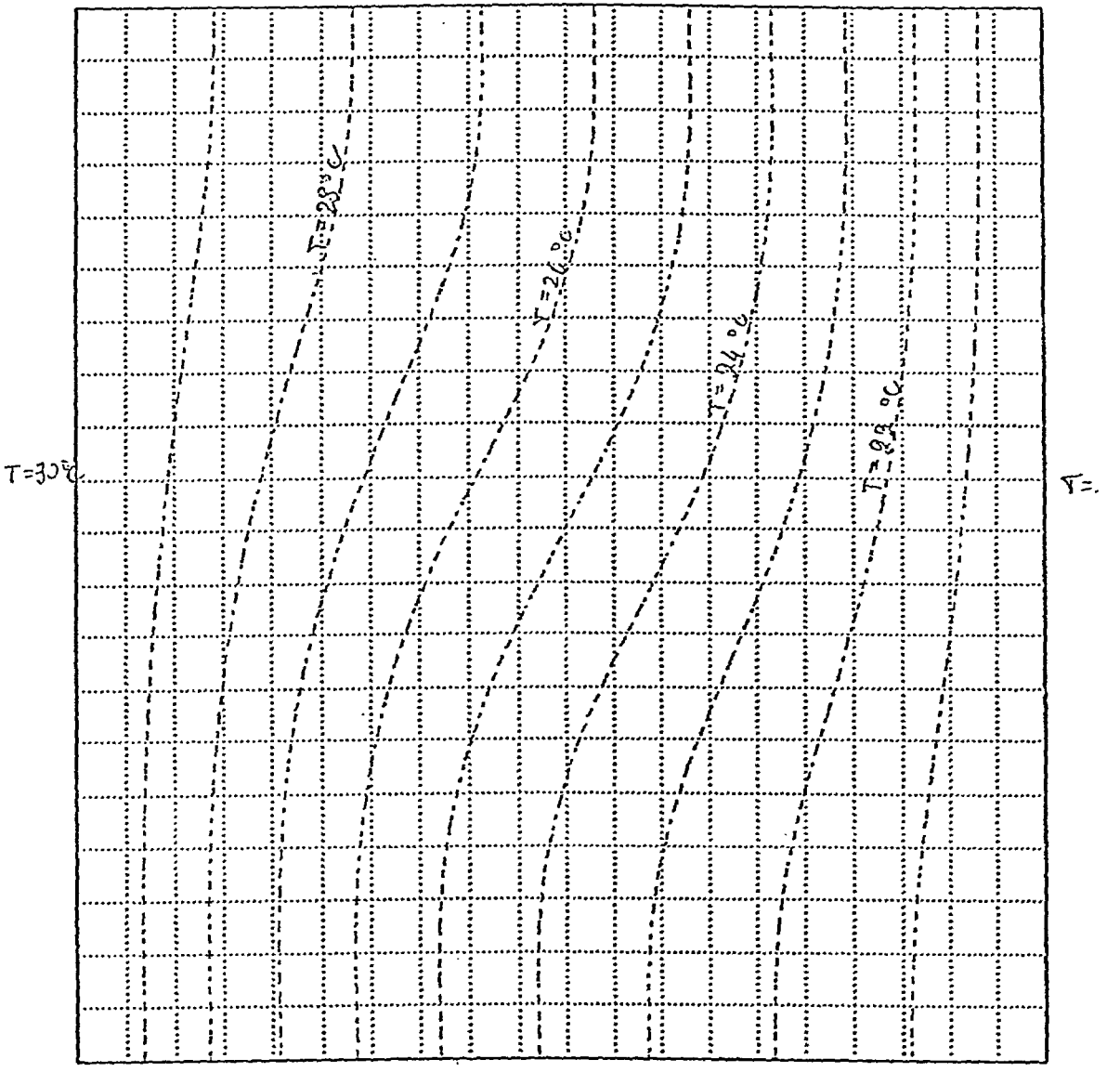

K = 1
Time: $2.39*10^3$ s

Case I: Plot FMa

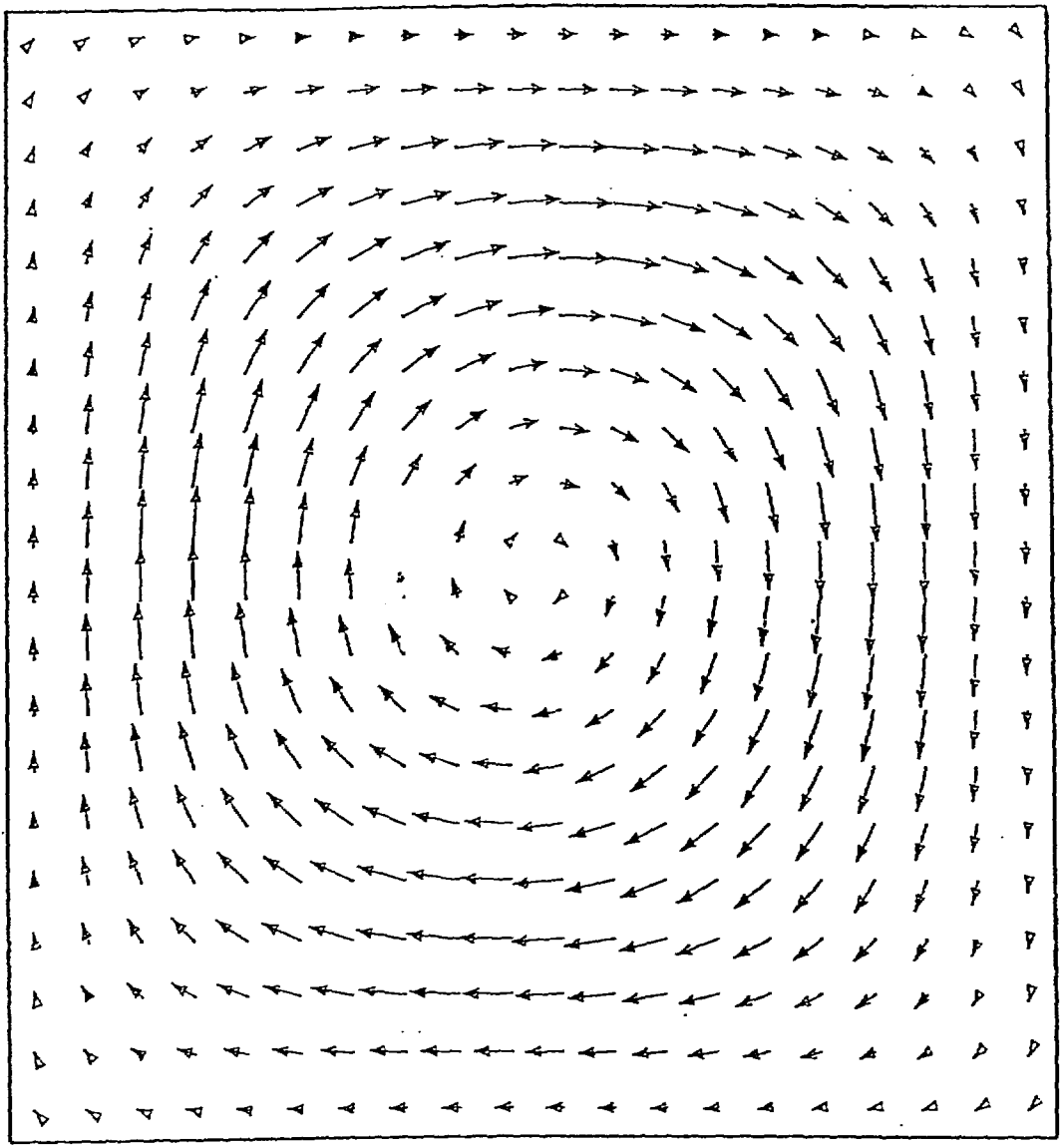

K = 1

$2.32*10^{-2}$ m/s

Time: $2.39*10^{3}$ s

Case I: Plot FMb

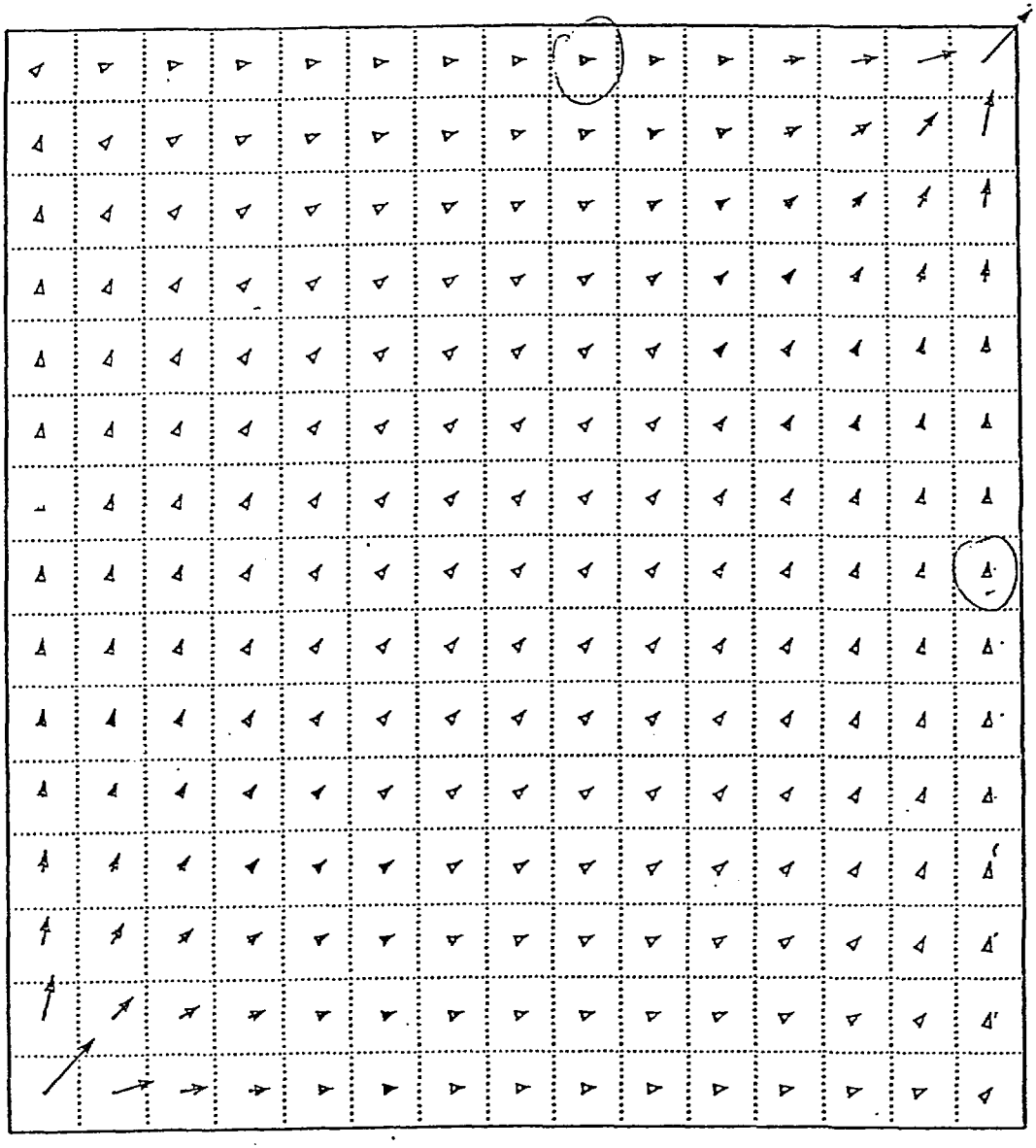

K = 1

3.26 m/s

Time: 72.00 s

Case II: Plot UPa

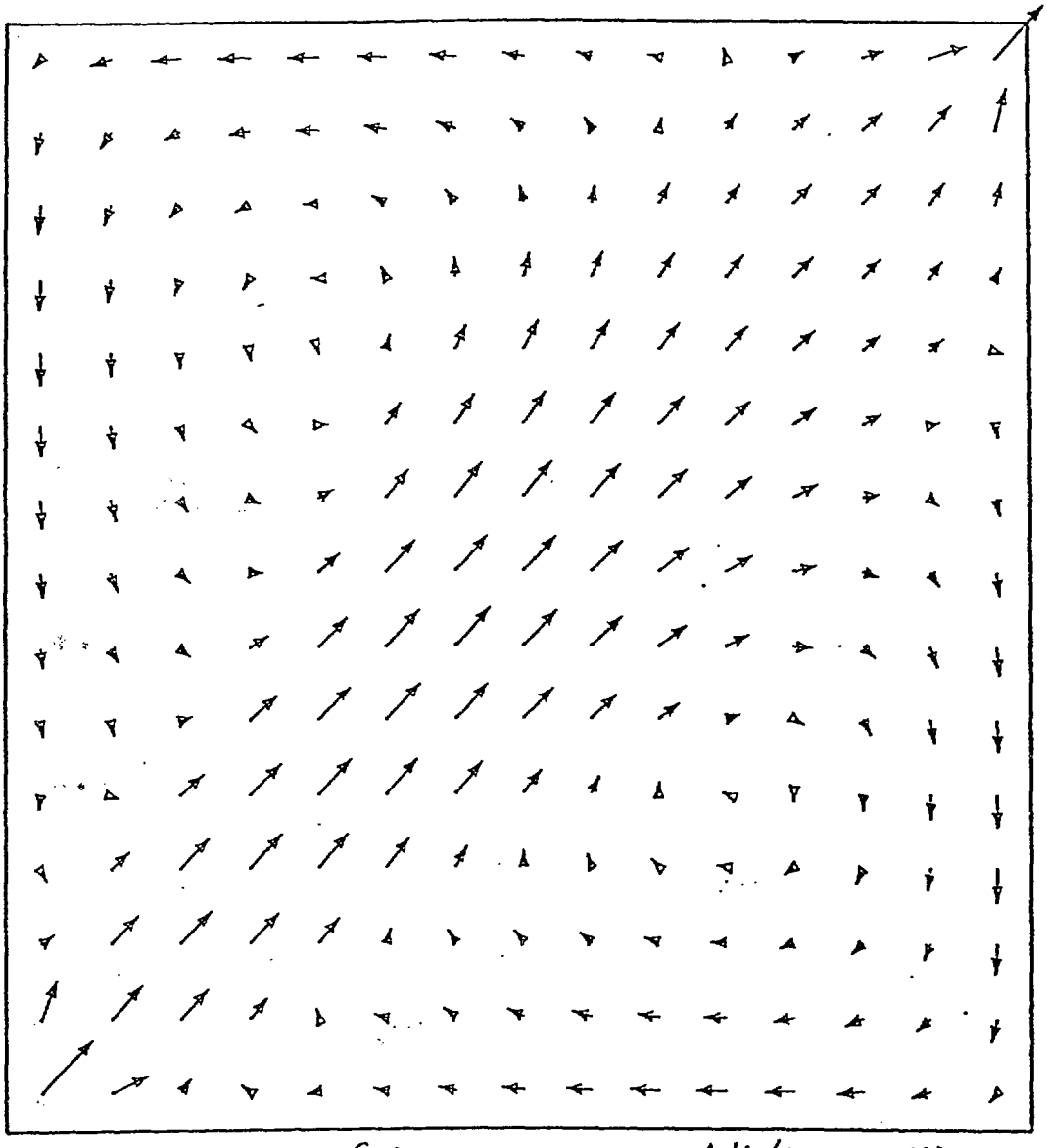

Case II: Plot FMa

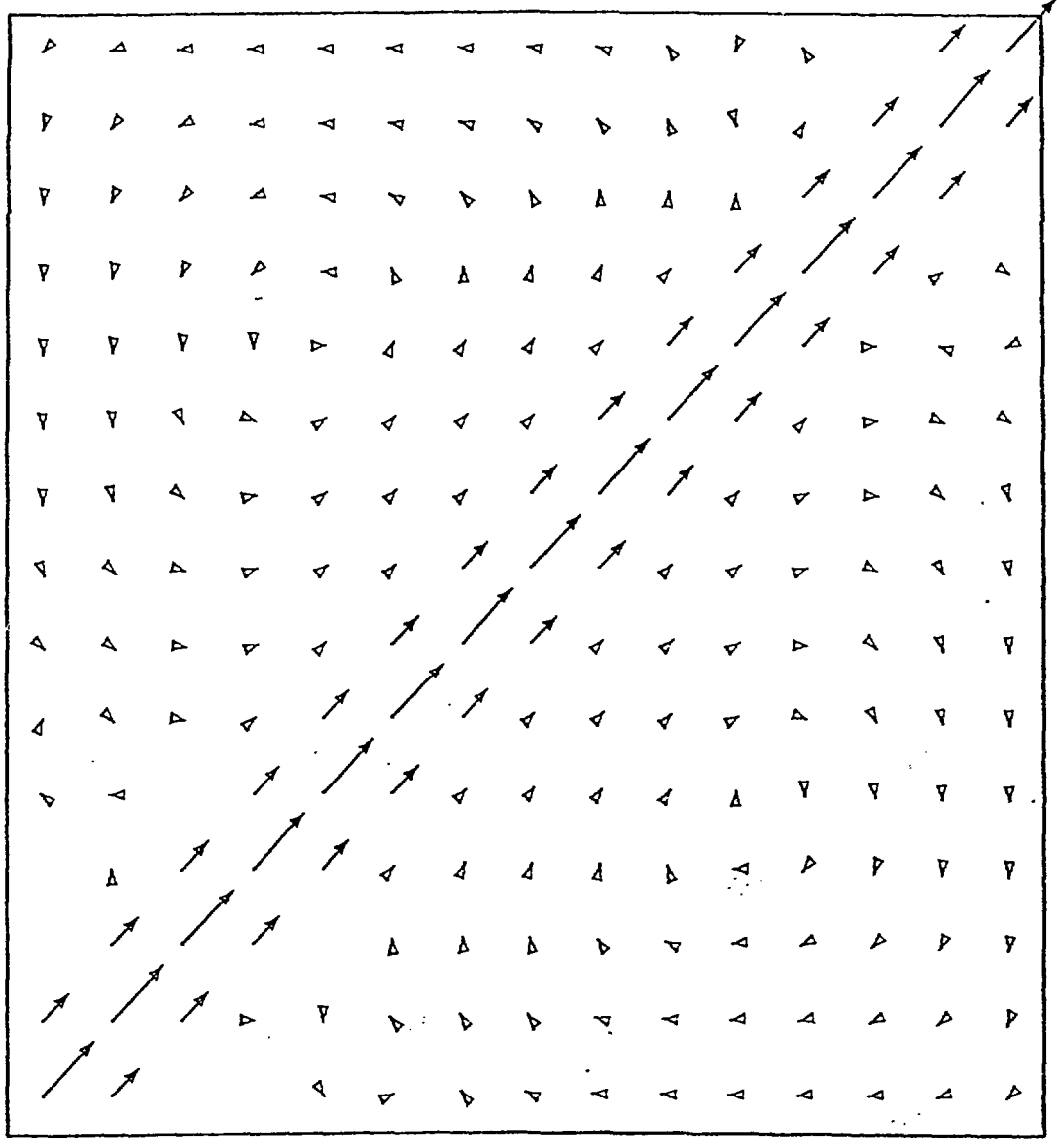

K = 1 (xy) - ω^2 & 11/10/90

3.27 m/s
Time: 60.00 s

Case II: Plot CTa

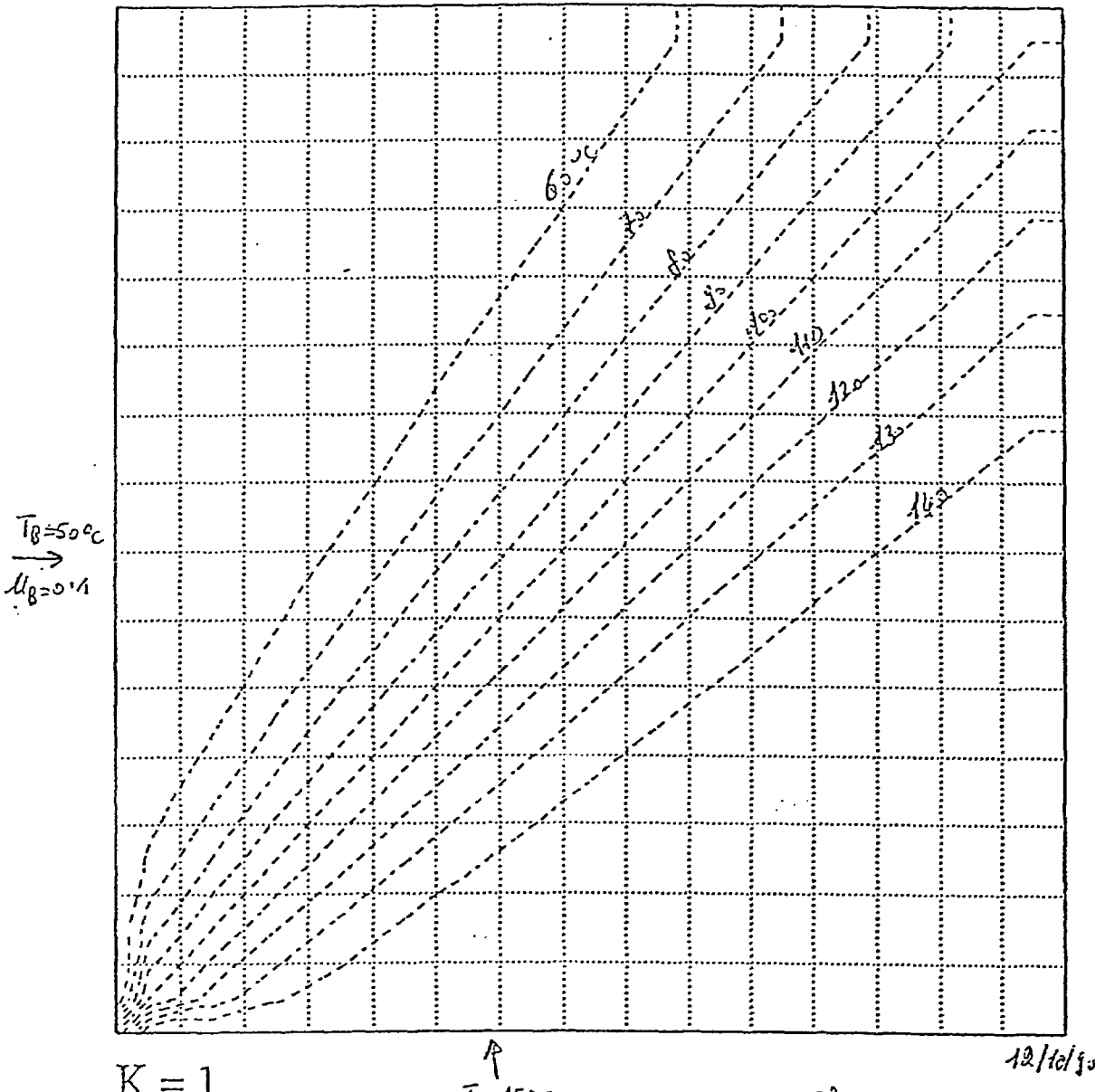

Case IV: Plot UPa

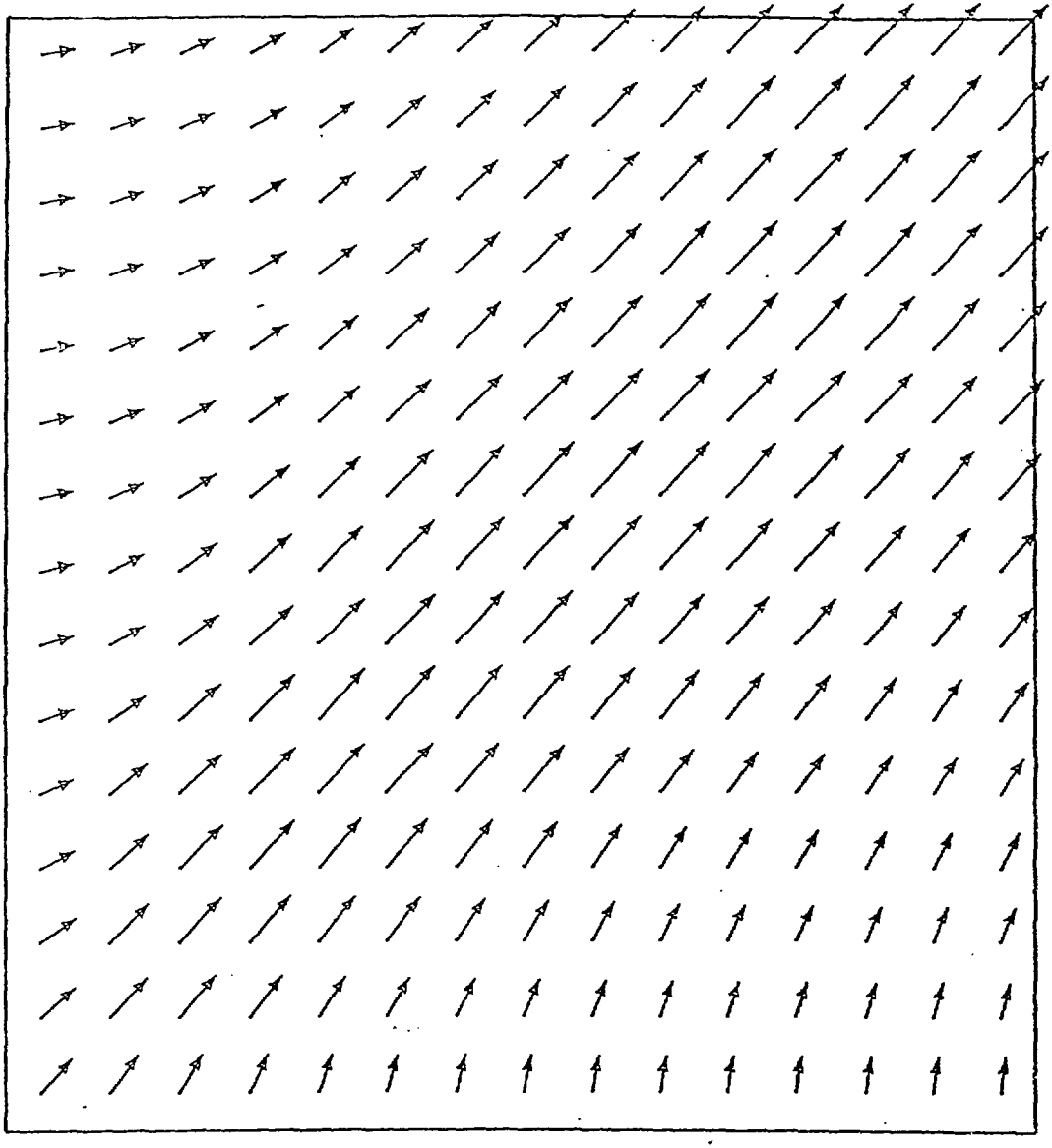

K = 1

0.52 m/s

Time: 63.00 s

Case IV: Plot UPb

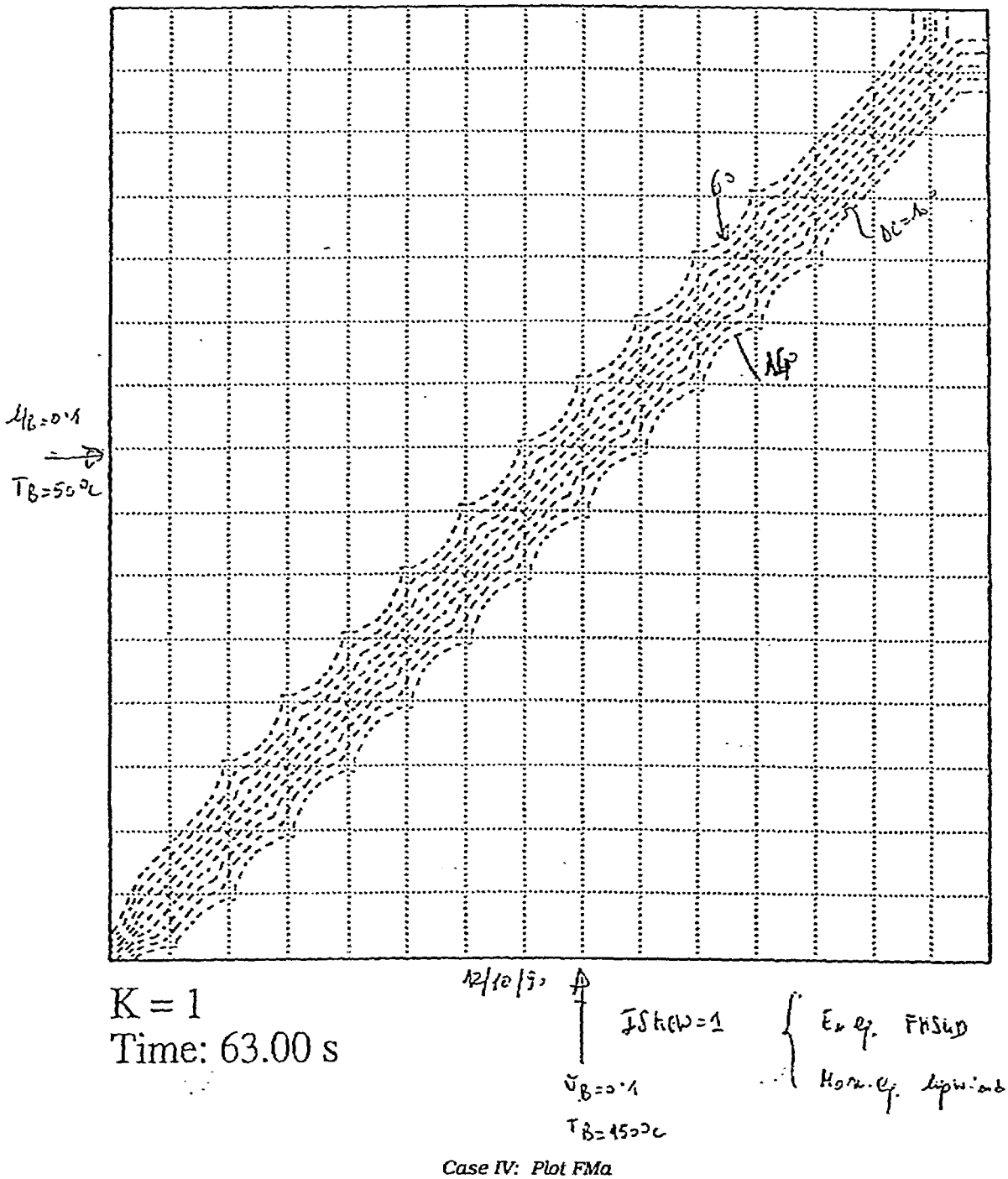

Case IV: Plot FMa

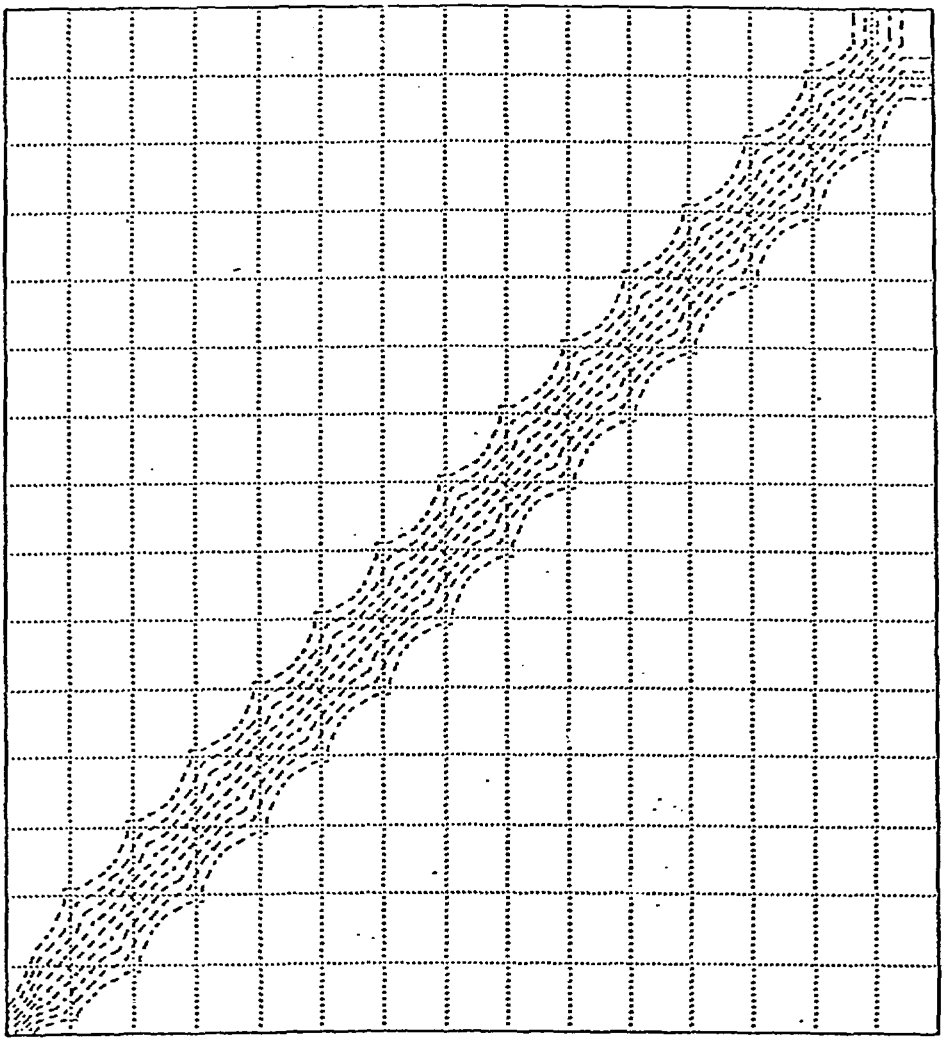

K = 1
Time: 55.00 s

13/10/90
Thermal.dat
ISKEW = 3
(Ex. eq ≡ FHSWD
Hex. eq ≡ (cos²θ) SWD)

Case IV: Plot CTa

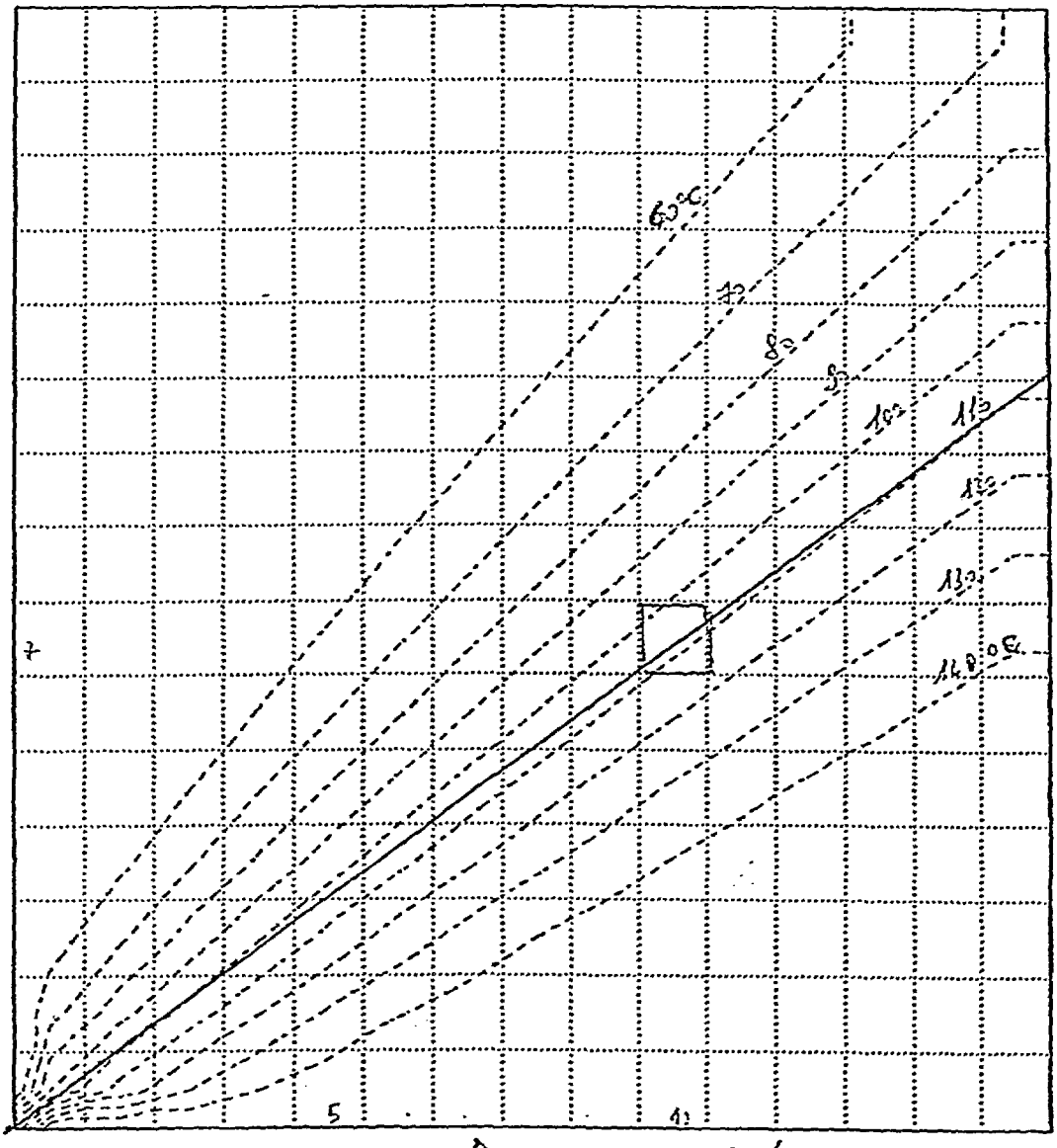

$\delta = 0.15$

$T_B = 50\ ^\circ C$

K = 1

Time: 62.00 s

$X_B = 0.10$

$T_B = 150\ ^\circ C$

(Upwind, $\Sigma = 0$)

23/10/92

Case V: Plot UPa

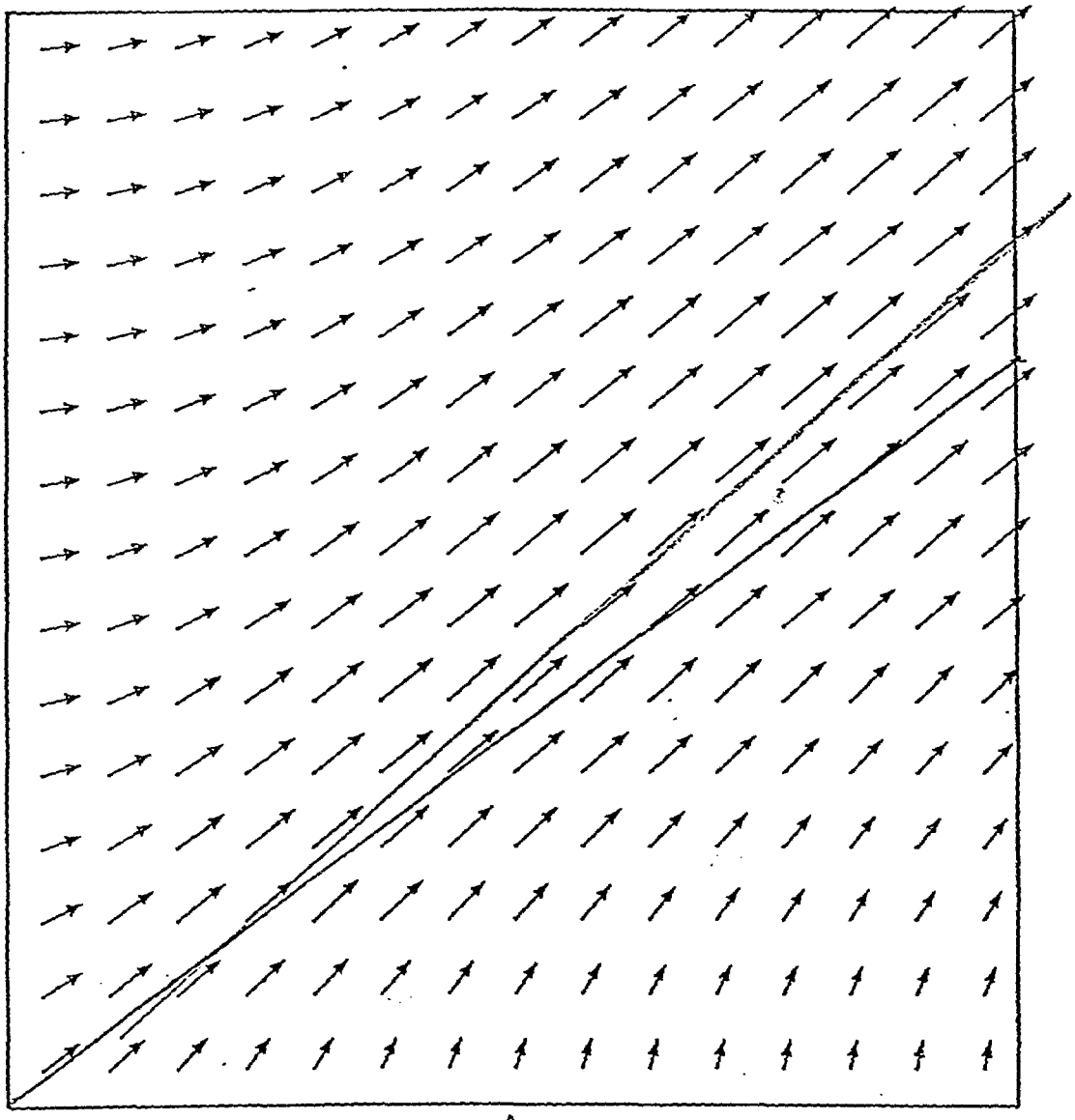

Case V: Plot UPb

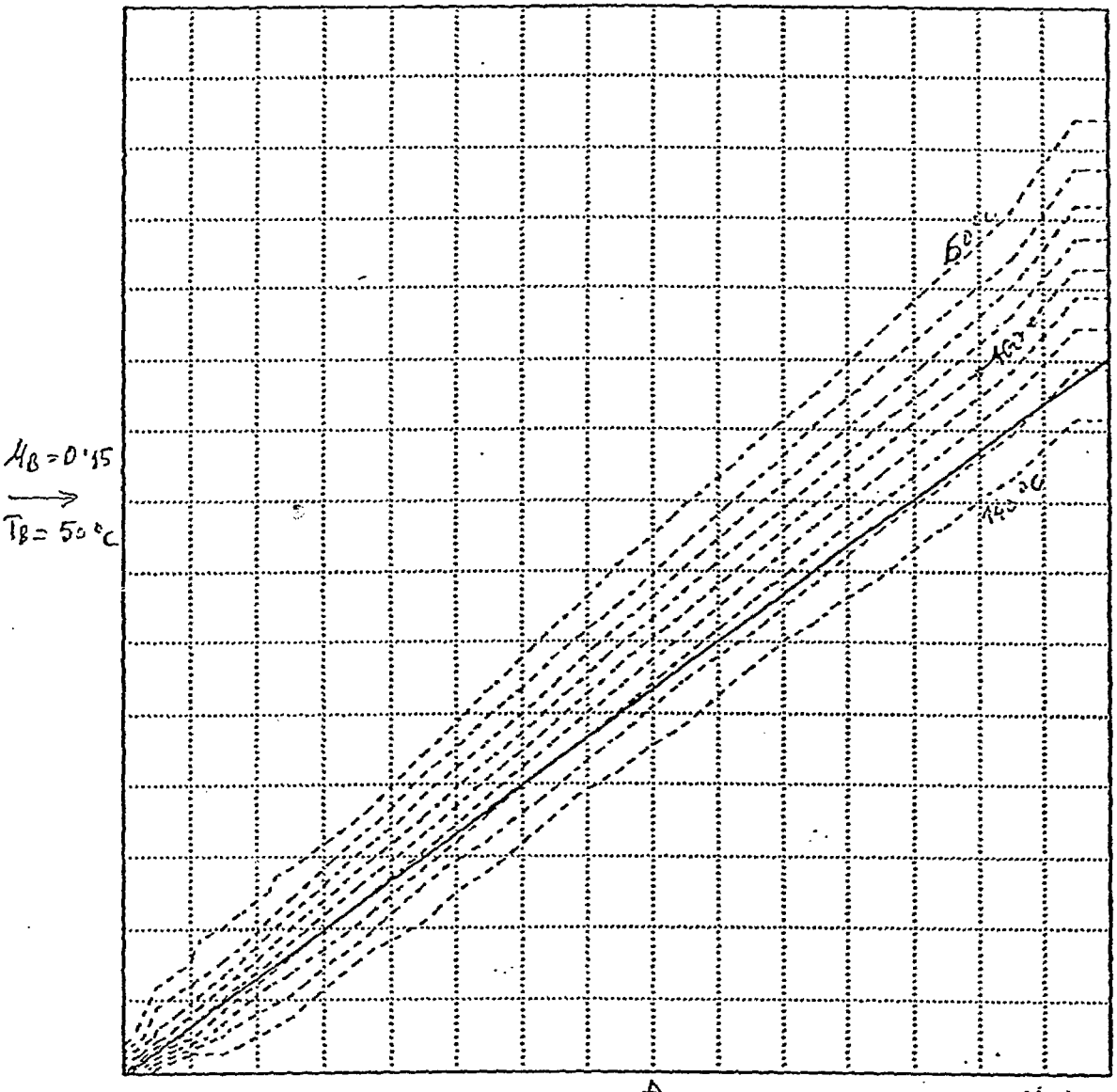

K = 1

Time: 62.00 s

FIXED (X) (Eq. = FH
Hom. Eq = upwind)

Case V: Plot UPc

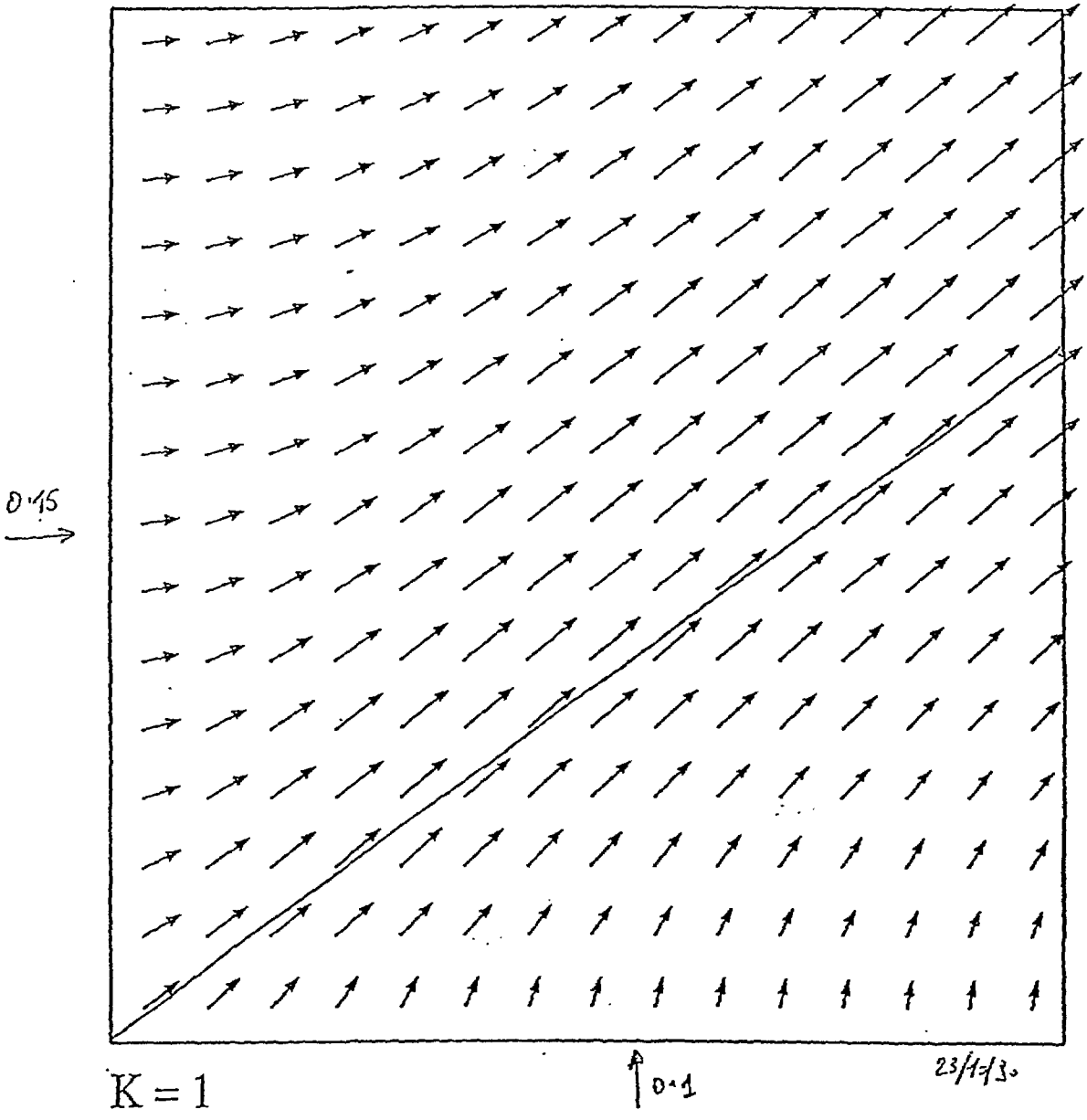

Case V: Plot UPd

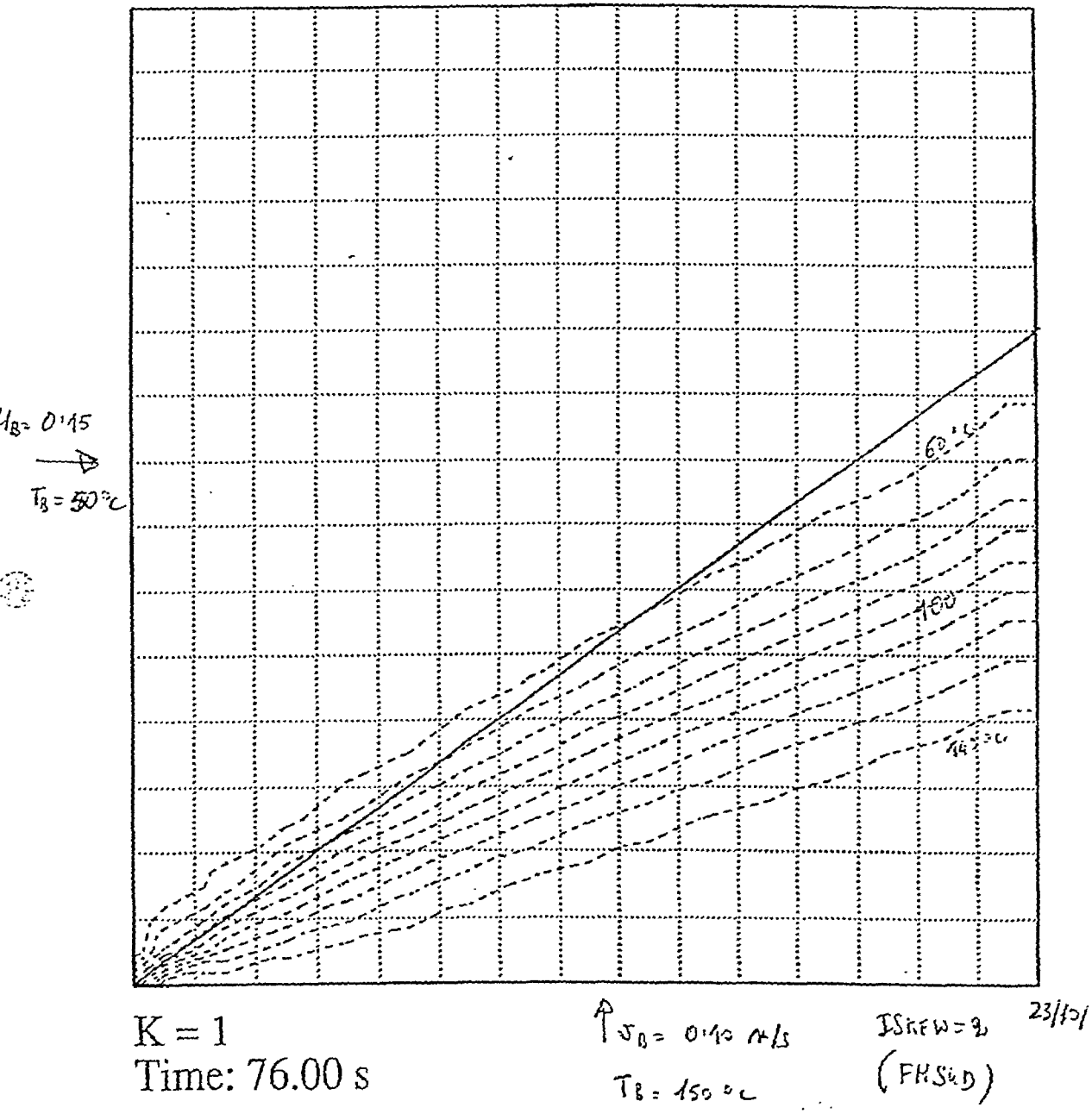

Case V: Plot FMa

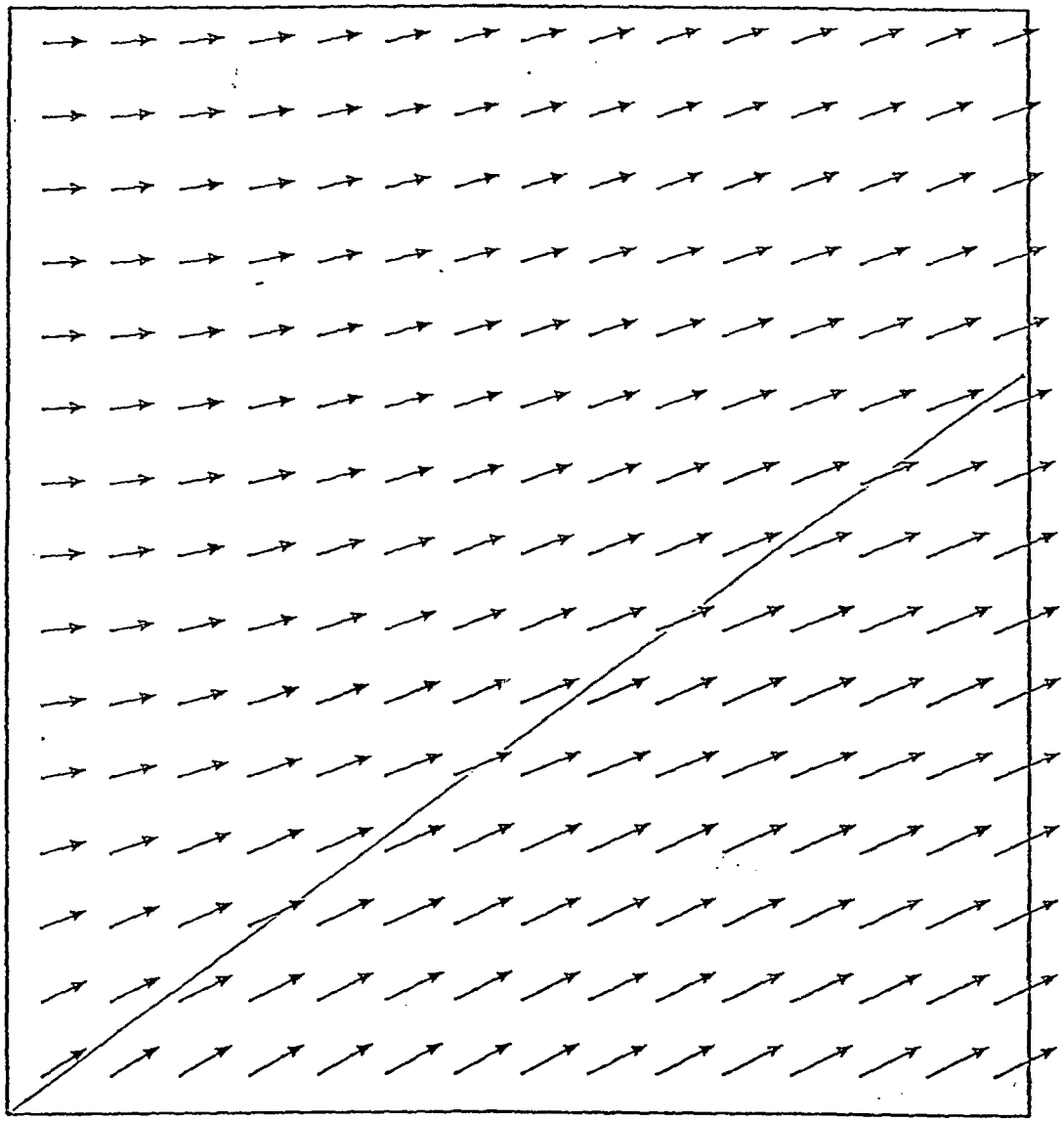

Case V: Plot FMb

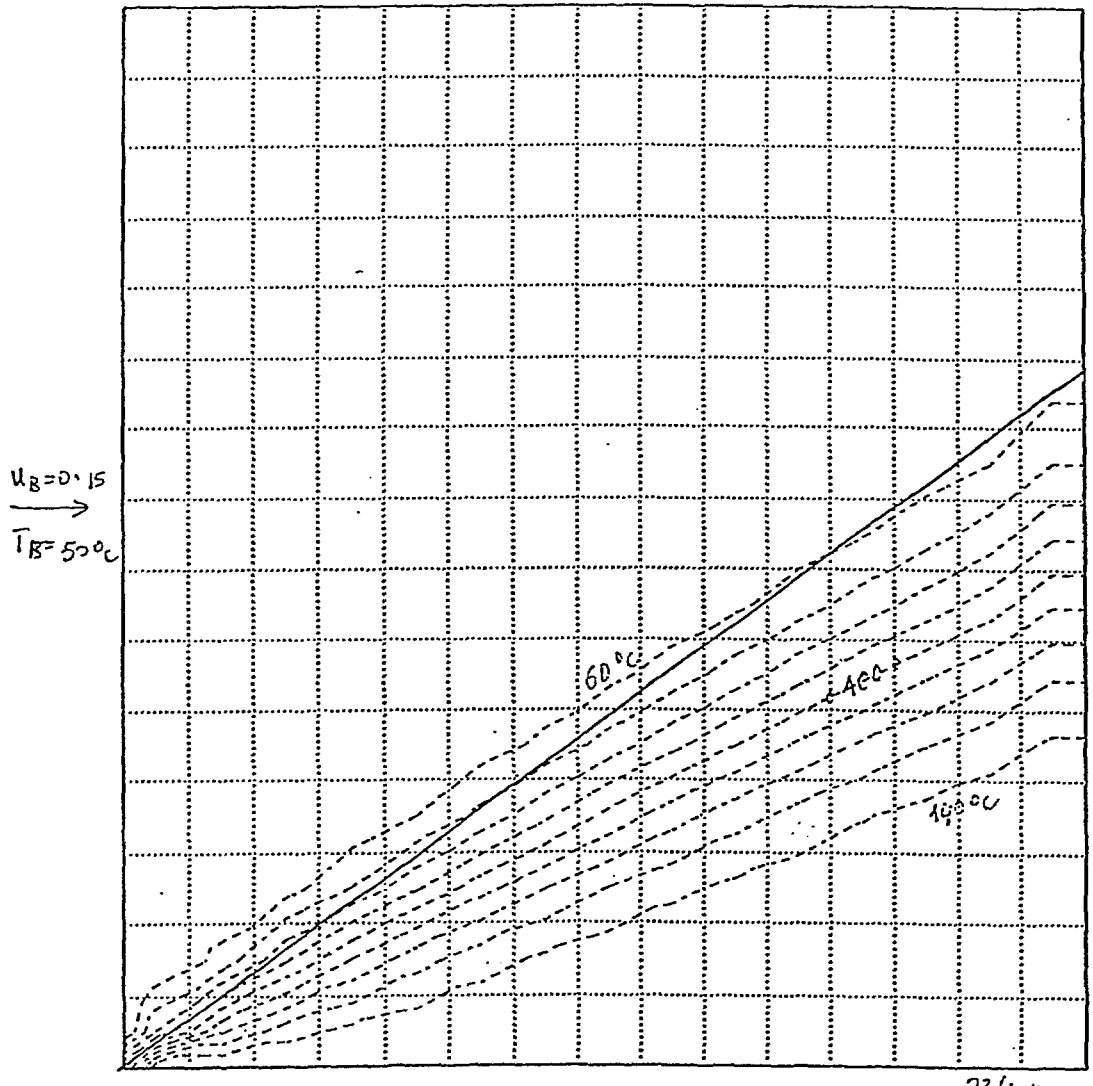

Case V: Plot CTa

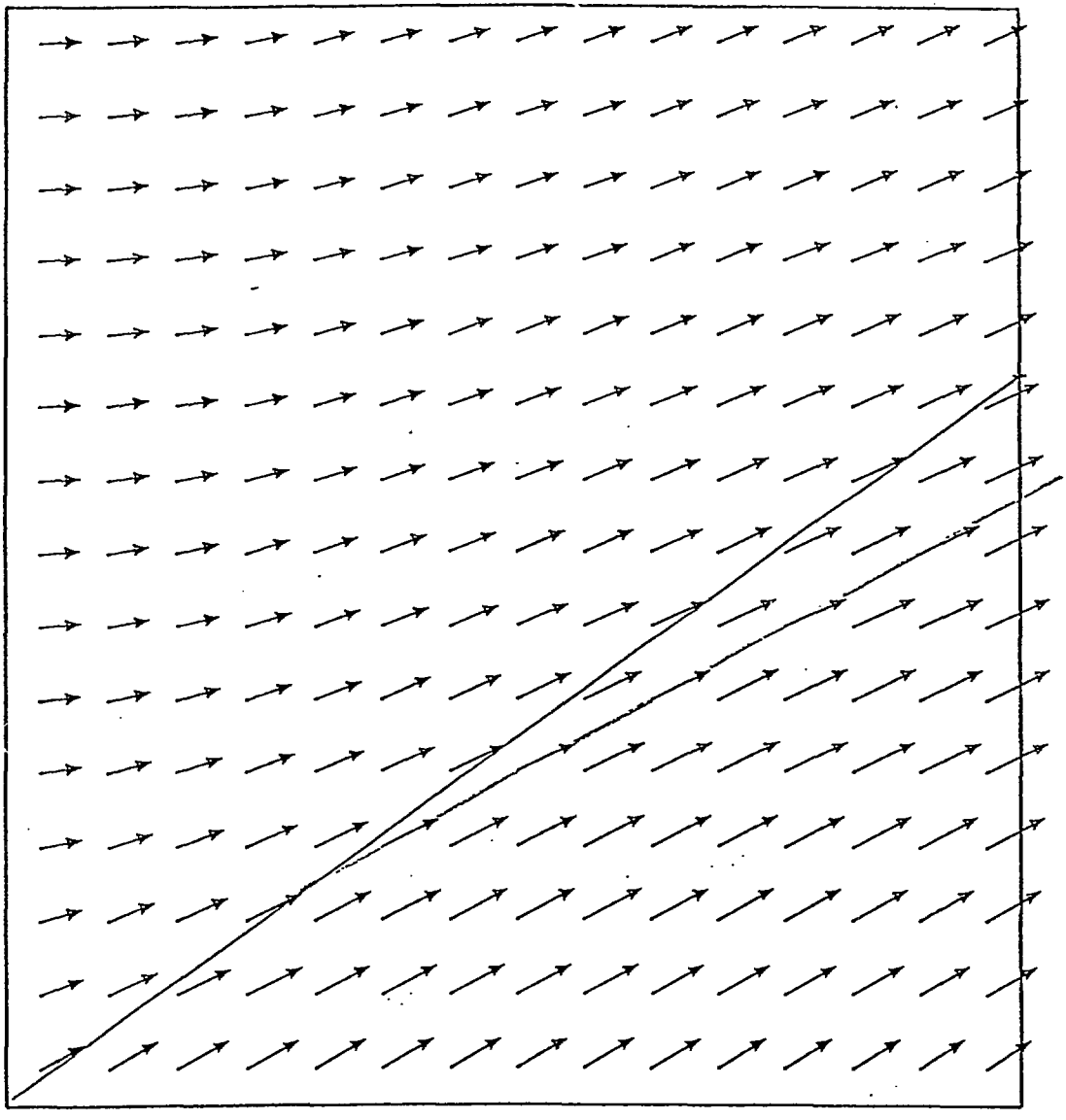

Case V: Plot CTb

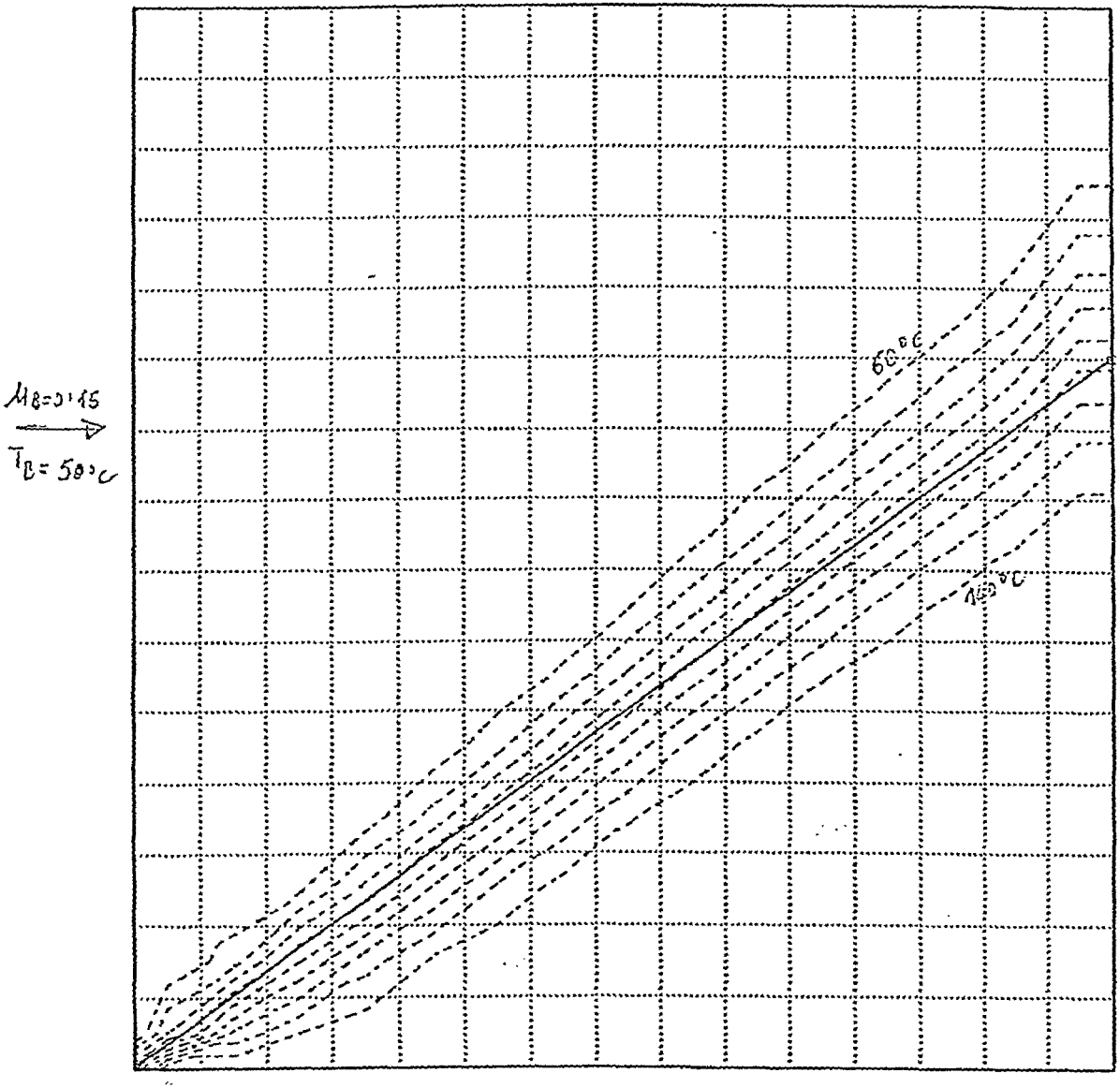

Case V: Plot CTc

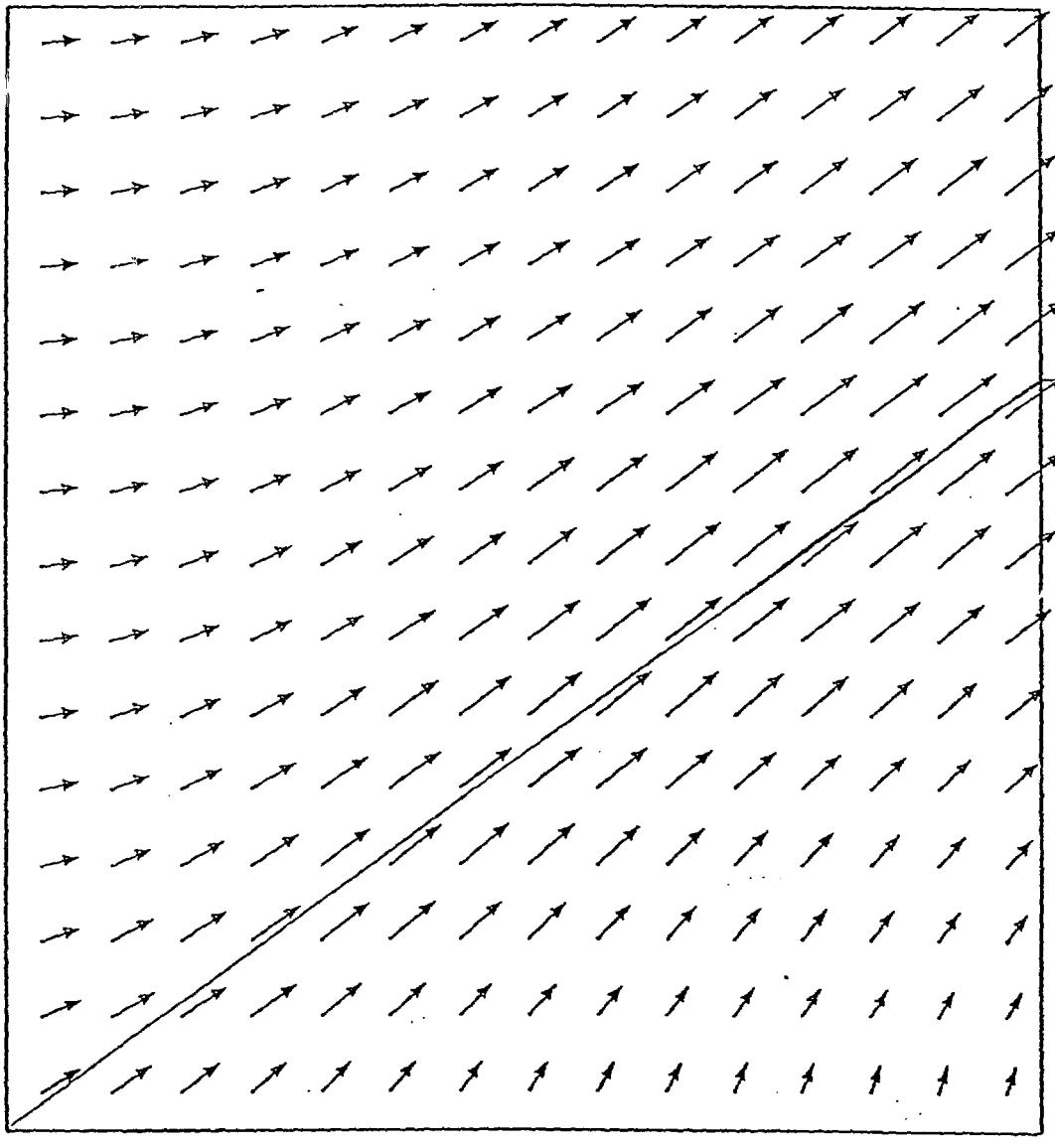

K = 1

0.71 m/s

Time: 65.00 s

Case V: Plot CTd